

Muonic Atoms. II. Isotope Shifts*

E. R. MACAGNO, S. BERNOW, S. C. CHENG, S. DEVONS, I. DUERDOTH,† D. HITLIN,‡ J. W. KAST

W. Y. LEE, J. RAINWATER, AND C. S. WU

Department of Physics, Columbia University, New York, New York 10027

AND

R. C. BARRETT

University of Surrey, Guildford, United Kingdom

(Received 10 November 1969)

Isotope shifts in the muonic spectra of $^{20}_{40}\text{Ca}$, ^{44}Ca ; $^{50}_{52}\text{Cr}$, ^{53}Cr , ^{54}Cr ; $^{29}_{63}\text{Cu}$, ^{65}Cu ; $^{42}_{92}\text{Mo}$, ^{95}Mo , ^{96}Mo , ^{97}Mo ; $^{50}_{118}\text{Sn}$, ^{117}Sn , ^{118}Sn , ^{119}Sn , ^{120}Sn , ^{122}Sn , ^{124}Sn ; $^{60}_{142}\text{Nd}$, ^{143}Nd , ^{144}Nd , ^{145}Nd , ^{146}Nd , ^{148}Nd , and ^{150}Nd have been measured using a stable high-resolution Ge(Li) spectrometer system. The results are compared with values calculated for assumed nuclear charge distributions. In the case of the Nd isotopes, the half-density radius and the skin thickness have been determined from the measured K and L x-ray energies. An interesting shell-closing effect has been observed among the Cr isotopes. The muonic isotope shifts have been used to extract specific-mass shifts from optical measurements. We find that, even in Nd, these specific-mass shifts are very large, and not at all negligible in the analysis of optical results. The isotope shifts in Sn follow favorably the theoretically predicted general trend. The great reduction of the isotope shift between $^{122}\text{--}^{124}\text{Sn}$ as reported in an optical investigation was not found in the muonic case. Lastly, a comparison has been made between the muonic results and recent electronic x-ray measurements. These were found to be in reasonable agreement.

I. INTRODUCTION

THE isotope shift of spectral lines due to the change of the nuclear charge distribution between isotopes was theoretically predicted in the early 1930's. Its usefulness as a sensitive means for revealing fine variations in nuclear structure as neutrons are added to a nucleus has made isotope shifts a major field of study. In the past four decades, optical spectroscopists have studied this effect in transitions of valence electrons with increasing intensity and ingenuity.¹ Measurements of isotope shifts in the spectra of muonic atoms, however, were not carried out until 1963.² A year later, preliminary electronic x-ray isotope-shift measurements were reported.³

The muonic and electronic x-ray methods have two clear advantages over the optical method. One is their greater sensitivity, due to the larger overlap of the muonic or $1s$ electron wave functions with the nucleus, and the other is the simplicity of the calculations, a consequence of the one-muon or innermost-electron nature of the system. However, these two methods are not without complications.

The interpretation of the electronic x-ray isotope shifts is relatively free from the limitations existing in the optical case. However, because of the line broadening, which is generally several hundred times larger than the line shift expected and, furthermore, because of the extreme sensitivity to chemical composition and crystalline structure, the experimental precision seems to be the major limitation to its effectiveness as a sensitive tool at the present moment. Both optical and electronic x-ray isotope-shift studies are limited to medium and heavy atoms with $Z \geq 40$. The radius of the electron orbit is long compared to the nuclear radius; therefore, the electron wave function can be considered to be constant over the nuclear volume. One can thus extract from these shifts only information on the change $\delta\langle r^{2\sigma'} \rangle$, where $\sigma' \cong 1 - 0.18Z^2\alpha^2$.

The muonic wavelength is comparable to or much smaller than the nuclear radius. For medium and heavy nuclei it is possible, in principle, to determine two parameters of the charge distribution if the absolute energies of K and L x rays are determined to an accuracy equal to or better than 1 and 0.2 keV, respectively. Under such favorable conditions, the isotope-shift results can be interpreted in terms of a Fermi charge distribution or other appropriate models, and the pairs of variations (δc and δt) or ($\delta\langle r^2 \rangle$ and δt) can be deduced. The $\delta\langle r^2 \rangle$ thus obtained in muonic atoms may then be compared with that obtained from optical and electronic x-ray results.

In optical spectra, although the shifts of δE between the isotopes are only a few parts in 10^6 of the transition energy, the experimental precision is better than $1:10^7$. The investigation can be carried out with minute quantities of materials (a sample as small as

* Work supported in part by the U.S. Atomic Energy Commission and the National Science Foundation.

† Present address: Physical Laboratories, The University, Manchester, England.

‡ Present address: SLAC, Stanford, California 94305.

¹ D. N. Stacey, Rept. Progr. Phys. **29**, 171 (1966), and references therein.

² H. L. Anderson, C. S. Johnson, E. P. Hincks, S. Raboy, and C. C. Trail, Phys. Letters **6**, 261 (1963); R. C. Cohen, S. Devons, A. D. Kanaris, and C. Nissim-Sabat, *ibid.* **11**, 70 (1964); J. A. Bjorkland, S. Raboy, C. C. Trail, R. D. Ehrlich, and R. J. Powers, Phys. Rev. **136**, B341 (1964).

³ R. T. Brockmeier, F. Boehm, and E. N. Hatch, Abstracts of the Symposium on Crystal Diffraction of Nuclear Gamma Rays, CALTECH, June 1964, p. 255.

10^{10} atoms has been used), hence even with short-lived radioactive isotopes. The accuracy of the theoretical evaluation of the spectra is limited. The isotope shift is proportional to the electron wave function at the nucleus, which can be estimated with an accuracy of $\sim 10\%$.

One of the useful roles of the muonic isotope shifts is to provide a normalization and calibration of the optical isotope shifts, particularly to extract the mass effects and thus facilitate the interpretation of the optical measurements.^{4,5}

In this paper, we present our results on isotope shifts in muonic atoms of Ca, Cr, Cu, Mo, Sn, and Nd. Some of these results were briefly reported previously.⁴⁻⁷

In the case of Ca, the reported abnormally small shift between $^{40-44}\text{Ca}$ was again confirmed. In Cr, the shell-closure effect for neutron number equal to 28 was observed. The isotope shift between $^{63-65}\text{Cu}$ is in good agreement with previously published results. In Mo, from the extracted mass effects, the observed *negative* optical shift between $^{96-97}\text{Mo}$ can be explained. The six pairs of tin isotopes, 116-117, 116-118, 118-119, 118-120, 120-122, 122-124, were thoroughly investigated. The results of the first five pairs of tin are in fair agreement with Ehrlich's work.⁸ The general trend of the variation is not at great variance with optical results. However, the shift between the pair 122-124 showed a marked departure from the optical result. The over-all trend of the muonic shifts in the Sn isotopes is in better accord with several theoretical predictions than the optical results. The isotope shifts in Nd were studied extensively for the pairs 142-143, 142-144, 144-145, 144-146, 146-148, 148-150. The absolute energies of the *K* and the *L* x rays were measured to a precision of $\simeq 0.50$ and $\simeq 0.15$ keV, respectively. From these measurements, with the inclusion of the nuclear-polarization and Lamb-shift corrections, we have determined the parameters *c* and *t* in the Fermi charge distribution of each isotope. The variations of *c* and *t* in Nd isotopes were determined by assuming either spherical nuclei or deformed nuclei with deformation parameter β determined from measured $B(E2)$ values. It is pertinent to note that the variation of *t* between the four even-even Nd isotope pairs does not exceed 4% (that is, $\delta t/t < 4\%$), and *t* can be considered constant within the experimental uncertainties. This evidence gives strong support to

the use of muonic x-ray results to extract the specific mass effects in the optical measurements of Nd.

To justify the application of the muonic isotope shifts to the normalization and calibration of the optical isotope shifts in general, a detailed examination and discussion of its conditions and limitations are presented. With the presently available precisions, this application can be made except in some anomalous cases.

Finally, comparisons between the muonic, electronic, and optical isotope shifts are made and discussed. The agreements among these various results are satisfactory.

II. INTERPRETATION OF MUONIC AND OPTICAL ISOTOPE SHIFTS: EXTRACTION OF THE SPECIFIC-MASS SHIFTS

A. Contributions to the Muonic Isotope Shifts

The precision which can be achieved in the measurement of muonic isotope shifts with present experimental techniques indicates that only transitions involving the $2p$, $2s$, or $1s$ levels will have measurable isotope shifts, even in heavy nuclei. (In ^{83}Bi , for example, the shift of the $3d$ levels is less than 50 eV between two isotopes differing by two neutrons.) Transitions which involve the $2s$ level, however, have such small intensities that with present facilities a very long time is required in order to achieve adequate precision.⁹ No isotope shifts of lines that include the $2s$ level have been measured.

In light nuclei, only the shifts of the $1s$ level are significant. In ^{20}Ca , for example, the standard ($A^{1/3}$ law) shift of the $2p$ levels is ~ 40 eV between isotopes differing by two neutrons. In muonic ^{60}Nd , however, the corresponding $2p$ isotope shift is ~ 600 eV, and therefore both the $1s$ level and the $2p$ level shifts can be measured. We will consider in our discussion (Sec. V) the significance of the measurement of the $2p$ level shifts.

Effects which contribute to the isotope shifts are:

a. The field effect. Changes in the extension or shape of the nuclear charge distribution from isotope to isotope give rise to shifts in the muonic levels. It is evident that the muon binding energy decreases as the volume occupied by the nuclear charge distribution increases.

The overlap of the muon wave function and the nuclear charge volume is different for each muonic state. The binding energy of each state, therefore, depends in a different manner upon the parameters of the nuclear charge distribution. In general, the

⁴ C. S. Wu, in *Proceedings of the International Conference on Nuclear Structure, Dubna 1967* (International Atomic Energy Agency, 1967); also in *Proceedings of the International Symposium on the Physics of One or Two Electron Atoms* (North Holland Publishing Co., Amsterdam, 1968).

⁵ C. S. Wu and L. Wilets, *Ann. Rev. Nucl. Sci.* **19**, 527 (1969).

⁶ E. R. Macagno *et al.*, *Bull. Am. Phys. Soc.* **12**, 75 (1967).

⁷ E. R. Macagno *et al.*, in *Proceedings of the International Conference on Electromagnetic Sizes of Nuclei, Ottawa, 1967* (Carleton University Press, Ottawa, Canada, 1968).

⁸ R. D. Ehrlich, *Phys. Rev.* **173**, 1088 (1968).

⁹ H. L. Anderson, C. K. Hargrove, E. P. Hincks, J. D. McAndrew, R. L. McKee, and D. Kessler, *Phys. Rev. Letters* **22**, 221 (1969).

radial moments of the charge distribution will take different values for different assumed distribution functions. It is of great interest to determine whether a transition actually determines *uniquely* some model-independent parameter or moment of the nuclear charge distribution.

Ford and Wills¹⁰ have shown this to be the case for Fermi and family II distributions. By carrying out exact numerical calculations with these spherically symmetric distribution functions, and considering reasonable variations of the parameters involved, they found that; (i) the energy of a muonic level or transition can be expressed to a high accuracy solely in terms of a moment $\langle r^k \rangle$ of the charge distribution, and (ii) the exponent k is a nearly linear function of Z for all transitions.

Defining the equivalent radius R_k as

$$R_k = [(3+k)/3\langle r^k \rangle]^{1/k}, \quad (1)$$

one can express the dependence of the energy upon the k th moment as

$$\delta E = (-1/C_Z)\delta R_k, \quad (2)$$

where C_Z is a function of Z and the transition involved, but not of the functional form of the distribution. For the Nd K x rays, for example,

$$k \simeq 1.13$$

and

$$C_Z \simeq 2.3 \text{ fm/MeV.}$$

Hence, it is possible to relate, in a unique manner, an isotope shift to a variation of the equivalent radius R_k .

As noted above, an isotope shift can originate from both a change in the nuclear volume and a change in the nuclear shape. It is a simple matter to show that the rms radius of a deformed nucleus is larger than the rms radius of a spherical nucleus of the same volume. The field-effect isotope shift between two isotopes with different volumes and deformations can be written as the sum of two parts,

$$(\delta E)_{\text{field}} = (\delta E)_{\text{volume}} + (\delta E)_{\text{deformation}}.$$

Note that the charge distributions considered by Ford and Wills¹⁰ in their analysis are all spherically symmetric. Because the deformation effects is of great importance, especially in Nd, where the isotopes vary from a closed-neutron-shell spherical nucleus (¹⁴²Nd) to a permanently deformed nucleus (¹⁵⁰Nd), we have not extracted from our experimental results numerical values of the k th moments, but have only used their results in a qualitative manner in our analysis.

b. Reduced-mass effect. The reduced mass of the

muon, which enters the Hamiltonian in the kinetic-energy term, varies with the nuclear mass. Hence the muonic energy levels would vary with the mass number A even if there were no change in the charge distribution, contributing additively to the isotope shifts. This effect can be readily calculated and has been taken into account in our results.

c. Vacuum polarization. To an increase in volume of the nuclear charge distribution corresponds a decrease in the vacuum-polarization contribution to the muonic-level energies. The effect on the isotope shifts is negligible for all but $1s$ level shifts. For example, between ¹⁴²Nd and ¹⁴⁴Nd the vacuum polarization in the $1s$ level decreases by 0.21 keV. Since the vacuum-polarization shift $\delta E_{v.p.}$ is to a good approximation directly proportional to the field-effect shift, we can write the isotope shift as

$$\begin{aligned} \delta E &= \delta E_{\text{field}} + \delta E_{v.p.} \\ &= \delta E_{\text{field}}(1 + \epsilon), \end{aligned} \quad (3)$$

where ϵ is the ratio of the vacuum-polarization shift to the field-effect shift, and $\epsilon \ll 1$. Moreover, for the same Z , ϵ is constant. It is apparent, therefore, that if the vacuum polarization is included in theoretical estimates of the isotope shift, then the quantity $(1 + \epsilon)$ cancels out when we take a ratio of experimental to theoretical isotope shifts. A similar cancellation obviously occurs when we take ratios of two experimental muonic shifts between different isotope pairs, as in our comparison with optical results. We will therefore neglect this effect.

d. Dynamic E2 effect. When the nucleus has low-lying collective excited states, as, for example, in the deformed rare earths, the muon-nucleus quadrupole interaction causes strong nuclear excitations.¹¹ This affects the energy of the $2p$ levels, but not the $1s$ level. Hence, this effect contributes to the shifts of transitions involving the $2p$ levels. As shown in Sec. IV, however, it is possible to determine the $1s$ level shift from a measurement of both K and L isotope shifts, thus avoiding the need to evaluate this dynamic E2 effect. On the other hand, in order to obtain absolute values of more than one parameter of the nuclear charge distribution, as well as for completeness, we have evaluated the corrections to the $2p$ levels in the Nd isotopes in the manner discussed in the preceding paper.¹² These corrections are given in Table I.

e. Nuclear polarization. This effect, discussed in the accompanying paper by Chen,¹³ depends upon details

¹¹ B. Jacobsohn, Phys. Rev. **96**, 1637 (1954); L. Wilets, Kgl. Danske Videnskab. Selskab, Mat.-Fys. Medd. **29**, No. 3 (1954).

¹² D. Hitlin, S. Bernow, S. Devons, I. Duerdoth, J. W. Kast, E. R. Macagno, J. Rainwater, C. S. Wu, and R. C. Barrett, preceding paper, Phys. Rev. C **1**, 1184 (1970).

¹³ M. Y. Chen, second preceding paper Phys. Rev. C **1**, 1176 (1970).

¹⁰ K. W. Ford and J. G. Wills, LASL Report No. LA-DC-10393, 1968 (unpublished).

of the structure of the nucleus. In heavy atoms, where the effect is largest, the $1s$ binding energy is increased by a few keV. To the extent that the level structure of a set of isotopes is similar, or can be assumed to be so, the isotopic variation of nuclear polarization is proportional to the variation in the overlap of the muon wave function and the nuclear charge, and hence, is negligible. This is the case for the nuclei we studied, except for the Nd isotopes. In this case, the low-lying level scheme and the $B(E2)$ values are known to vary smoothly from the spherical ${}_{60}^{142}\text{Nd}$ to the strongly deformed ${}_{60}^{150}\text{Nd}$ (90 neutrons is the onset of strong deformation). Chen¹⁴ has calculated the isotopic variation of the nuclear polarization in Nd by considering only the lowest (2^+) nuclear levels. His results are given in Table II. Much more information about the level structure in the Nd isotopes is required before a complete calculation can be carried out.

f. Lamb shift. The Lamb shift in muonic atoms has been recently calculated by Barrett.¹⁵ In Nd, he calculated a decrease in the binding energy of the $1s_{1/2}$ state of 2.3 keV. The isotopic variation, about 0.5%, is negligible. We have, however, included this effect in our analysis of the absolute energies in the Nd isotopes. The values are given in Table II.

Taking these various terms into account, we can write the following expression for the experimental isotope shift:

$$(\delta E)_{\text{exp}} = (\delta E)_{\text{field}} + (\delta E)_{\text{r.m.}} + (\delta E)_{\text{n.p.}}, \quad (4)$$

where the terms on the right arise from the field effect, the reduced-mass effect and the nuclear-polarization differences, respectively.

It is customary to compare the term $(\delta E)_{\text{field}}$ obtained from the experimental value, with the value for this term as calculated for the model of a uniformly charged spherical nucleus with radius $R = 1.2A^{1/3}$ F. The value of $(\delta E)_{\text{field}}$ so calculated is known as the standard isotope shift, $(\delta E)_{\text{std}}$.

TABLE I. Shift of the $2p$ muonic levels in the Nd isotopes by the dynamic quadrupole interaction. The shifts increase the muon binding energy.

Isotope	$\delta E(2p_{1/2})$ (keV)	$\delta E(2p_{3/2})$ (keV)
${}^{142}\text{Nd}$	0.10	0.11
${}^{144}\text{Nd}$	0.31	0.36
${}^{146}\text{Nd}$	0.67	0.87
${}^{148}\text{Nd}$	1.70	2.56
${}^{150}\text{Nd}$	6.64	17.93

¹⁴ M. Y. Chen (private communication).

¹⁵ R. C. Barrett, Phys. Letters **28B**, 93 (1968).

TABLE II. Lamb-shift and nuclear-polarization corrections to muonic levels in the Nd isotopes. The Lamb shift decreases the muon binding energy, and the nuclear polarization increases it.

Isotope	Level	Lamb shift (keV)	Nuclear polarization (keV)	Total correction (keV)
${}^{142}\text{Nd}$	$1s_{1/2}$	-2.30	4.25	1.95
	$2p_{1/2}$	-0.16	0.70	0.54
	$2p_{3/2}$	-0.29	0.70	0.41
${}^{144}\text{Nd}$	$1s_{1/2}$	-2.30	4.44	2.14
	$2p_{1/2}$	-0.16	0.76	0.60
	$2p_{3/2}$	-0.29	0.76	0.47
${}^{146}\text{Nd}$	$1s_{1/2}$	-2.30	4.76	2.46
	$2p_{1/2}$	-0.16	0.85	0.69
	$2p_{3/2}$	-0.29	0.85	0.56
${}^{148}\text{Nd}$	$1s_{1/2}$	-2.30	5.40	3.10
	$2p_{1/2}$	-0.16	1.06	0.90
	$2p_{3/2}$	-0.29	1.06	0.77
${}^{150}\text{Nd}$	$1s_{1/2}$	-2.30	6.90	4.60
	$2p_{1/2}$	-0.16	1.53	1.37
	$2p_{3/2}$	-0.29	1.53	1.24

B. Analysis of Measured Muonic X-Ray Energies

We have analyzed the measured transition energies in the Nd isotopes in terms of the two-parameter Fermi distribution,

$$\rho(r) = \rho_0 \left\{ 1 + \exp \left[\frac{(r-c)}{0.228t} \right] \right\}^{-1}, \quad (5)$$

where c and t are the half-density radius and the skin-thickness parameter, and a three-parameter modified Fermi distribution,

$$\rho(r) = \rho_0 \left\{ 1 + \exp \left[\frac{r-c(1+\beta Y_{20}(\theta, \phi))}{0.228t} \right] \right\}^{-1}, \quad (6)$$

where β is the deformation parameter. The values of β were derived from $B(E2)$ measurements.^{16,17} We have taken into account in the analysis the dynamic $E2$, Lamb shift,¹⁵ and nuclear-polarization corrections¹⁴ given in Tables I and II. The procedure used to determine the values of the parameters and the errors is described in the previous paper.¹²

¹⁶ P. H. Stelson and L. Grodzins, Nucl. Data **1A**, 21 (1965).

¹⁷ P. A. Crowley, J. X. Saladin, J. E. Glenn, J. R. Kerns, and R. J. Pryor, Bull. Am. Phys. Soc. **13**, 79 (1968).

C. Comparison of Muonic and Optical Isotope Shifts: Extraction of the Specific-Mass Term

1. Review of Optical Isotope Shifts

The optical isotope shift can be written as the sum of three terms,

$$\delta E = (\delta E)_{\text{field}} + (\delta E)_{\text{r.m.}} + (\delta E)_{\text{s.m.}} \quad (7)$$

The first two terms are analogous to those in Eq. (4) for the muonic isotope shift. The third is the so-called "specific-mass shift." If the kinetic energy of the atom is written in the c.m. coordinates, it can be separated into two terms,

$$(1/2\mu) \sum_{j=1}^n (\mathbf{P}_j)^2 + (1/2M) \sum_{j \neq i} (\mathbf{P}_j \cdot \mathbf{P}_i), \quad (8)$$

where μ is the electron reduced mass, M is the nuclear mass, \mathbf{P}_j is the momentum of the j th electron, and the sum is over all electrons. The isotopic variations of μ in the first term gives rise to the reduced-mass shift $(\delta E)_{\text{r.m.}}$; the difference in M in the second term gives rise to the specific-mass shift $(\delta E)_{\text{s.m.}}$.

Whereas it is quite trivial to evaluate the reduced-mass shift, this is not the case for the specific-mass term in that it is necessary to know the (many-body) correlations between all the electrons in the atom in order to calculate this specific-mass effect. Such calculations are very involved. Since a knowledge of the specific-mass shift is necessary prior to the extraction of the field-effect shift $(\delta E)_{\text{field}}$, it is apparent that a severe limitation exists in the interpretation of optical-isotope-shift measurements in the heavier nuclei.

It is of interest to note that in the early analysis of the optical isotope shift in heavy nuclei, the fact that the specific-mass term is proportional to the inverse nuclear mass squared was taken to imply that the term was negligible for elements of $A > 60$.¹ An investigation of the ${}_{60}\text{Sm}$ isotopes by Striganov *et al.*¹⁸ in 1961, however, revealed that relative isotope shifts for some lines were quite different than for other lines. This peculiarity was explained by King¹⁹ by suggesting that very large specific-mass shifts (some six times the reduced-mass shift) were present. As will be shown below, we also find from our analysis that there are large specific mass shifts in ${}_{60}\text{Nd}$.

Since the electron wave-function is quite constant over the nuclear dimensions, it can be shown that the field-effect term depends only on the change in the $2\sigma'$ radial moment ($\sigma' = 1 - 0.18Z^2\sigma^2$) of the nuclear charge distribution in a model-independent manner.²⁰ The rest of this term contains electronic factors, especially so-called "screening" effects: When the

valence electron undergoes a transition, the shielding by this electron of the other electrons changes. This affects the magnitude of the shift by up to 20%, but with an uncertainty in the calculation of about 10%.¹

In principle, the nuclear polarization also contributes to the measured optical isotope shifts. Reiner and Wilets,²¹ however, have shown this effect to be negligible.

In general, the mass shifts dominate for $Z < 40$, and therefore few measurements are made for lighter nuclides. For medium and heavy atoms, the mass effects still play a very important role and an accurate determination of them by any means would be desirable.

2. Determination of Specific-Mass Shifts

In cases where the isotope shifts between two or more pairs of isotopes have been measured in both muonic and optical transitions, the muonic results can be used to determine the specific-mass shifts, provided that the difference in nuclear-polarization effects is either small or can be taken into account.

Since the reduced-mass shift can be readily subtracted, we will assume in the following that the measured shifts have already been so corrected.

The specific-mass shift can be written as

$$(\delta_{12}E)_{\text{s.m.}} = [(A_2 - A_1)/A_1A_2]C, \quad (9)$$

where A_1 , A_2 are the mass numbers of the isotopes and C , called the specific-mass constant, is independent of the nuclear masses but can take different values for different transitions. The field-effect shift is given by

$$(\delta_{12}E)_{\text{field}} = FV(A_1, A_2), \quad (10)$$

where F contains all electronic factors (including screening) and $V(A_1, A_2)$ depends only upon the nuclear charge distributions of the two isotopes. Hence, the measured optical isotope shift can be written as

$$(\delta_{12}E)_{\text{opt}} = FV(A_1, A_2) + [(A_2 - A_1)/A_1A_2]C. \quad (11)$$

If the isotope shift from another pair of isotopes, A_3 and A_4 , has been measured for the same transition, we can eliminate the electronic factor F by forming the ratio

$$\begin{aligned} [(\delta_{12}E)_{\text{opt}} - a_{12}C] / [(\delta_{34}E)_{\text{opt}} - a_{34}C] \\ = V(A_1, A_2) / V(A_3, A_4), \quad (12) \end{aligned}$$

where we have set $a_{ij} = (A_j - A_i)/A_iA_j$. Since $V(A_1, A_2) \sim \delta_{12}\langle r^2 \rangle$ (to be more exact, $\delta_{12}\langle r^2 \rangle$ should be replaced by $\delta_{12}\langle r^{2\sigma'} \rangle$), it follows that

$$[(\delta_{12}E)_{\text{opt}} - a_{12}C] / [(\delta_{34}E)_{\text{opt}} - a_{34}C] = \delta_{12}\langle r^2 \rangle / \delta_{34}\langle r^2 \rangle. \quad (13)$$

For the muonic case, we obtain the ratio (as in the

¹⁸ A. R. Stringanov, V. A. Katulin, and V. V. Eliseev, *Opt. i Spektroskopiya* **12**, 171 (1961) [English transl.: *Opt. Spectry*, (USSR) **12**, 91 (1962)].

¹⁹ W. H. King, *J. Opt. Soc. Am.* **53**, 638 (1963).

²⁰ A. R. Bodmer, *Nucl. Phys.* **9**, 371 (1959).

²¹ A. S. Reiner and L. Wilets, *Nucl. Phys.* **36**, 457 (1962).

paper by Wu and Wilets⁵)

$$(\delta_{12}E)_\mu / (\delta_{34}E)_\mu = \delta_{12} \langle r^k \rangle / \delta_{34} \langle r^k \rangle, \quad (14)$$

where k is the effective-moment parameter defined by Ford and Wills¹⁰ [see Eq. (1)].

If the nuclear charge distribution were uniform, then we would be justified in equating the ratios (13) and (14) (see Ref. 5):

$$\delta_{12} \langle r^k \rangle / \delta_{34} \langle r^k \rangle \approx \delta_{12} \langle r^2 \rangle / \delta_{34} \langle r^2 \rangle. \quad (15)$$

In order to determine how accurate this identification is in general, we must consider a more realistic nuclear charge distribution, such as the Fermi distribution [Eq. (5)]. In terms of the parameters c and t ,

$$\delta \langle r^k \rangle = \alpha_k \delta c + \beta_k \delta t,$$

where

$$\alpha_k = \int (\partial \rho / \partial c) r^k dx,$$

$$\beta_k = \int (\partial \rho / \partial t) r^k dx.$$

Then if the ratio

$$\begin{aligned} \mathcal{R} &= \frac{\delta_{12} \langle r^2 \rangle / \delta_{34} \langle r^2 \rangle}{\delta_{12} \langle r^k \rangle / \delta_{34} \langle r^k \rangle} \\ &= \frac{(\alpha_2 \delta_{12} c + \beta_2 \delta_{12} t) / (\alpha_2 \delta_{34} c + \beta_2 \delta_{34} t)}{(\alpha_k \delta_{12} c + \beta_k \delta_{12} t) / (\alpha_k \delta_{34} c + \beta_k \delta_{34} t)} \end{aligned} \quad (16)$$

is close to unity, Eq. (15) is justified. It is of interest to note that $\mathcal{R} \equiv 1$ in the following special cases:

- (a) $\delta_{12} t = \delta_{34} t = 0$,
- (b) $\delta_{12} c = \delta_{34} c = 0$,
- (c) $\delta_{12} t / \delta_{12} c = \delta_{34} t / \delta_{34} c$.

In general, however, \mathcal{R} can deviate somewhat from unity, as discussed below.

To obtain some feeling for the dependence of \mathcal{R} on δc and δt , let us consider $\alpha \delta c \gg \beta \delta t$. Then

$$\mathcal{R} \approx 1 + (\beta_2 / \alpha_2 - \beta_k / \alpha_k) (\delta_{12} t / \delta_{12} c - \delta_{34} t / \delta_{34} c). \quad (17)$$

For $Z=60$ (Nd), $k=1.14$, $c \approx 6$ fm, $t \approx 2$ fm and choosing $\delta_{12} c = \delta_{34} c = 0.03$ fm,

$$\mathcal{R} \approx 1 + 2.5 (\delta^2 t / t), \quad (\delta^2 t = \delta_{12} t - \delta_{34} t).$$

In this case, relative fluctuations of t are amplified by a factor of 2.5, which is not serious provided $\delta^2 t \ll t$. As an extreme example, let $\delta_{34} t = 0$. Then Eq. (16) becomes

$$\mathcal{R} = \frac{1 + (\beta_2 / \alpha_2) (\delta_{12} t / \delta_{12} c)}{1 + (\beta_k / \alpha_k) (\delta_{12} t / \delta_{12} c)}. \quad (18)$$

In the limit that $(\beta \delta t) \gg 1$,

$$\mathcal{R} = \frac{\beta_2 / \alpha_2}{\beta_k / \alpha_k} \sim \frac{7}{k+5}$$

which is equal to 1.14 for Nd, where $k=1.14$.

If $\delta t / \delta c$ is negative, the isotope shifts can be small, or close to zero. Very small optical and muonic shifts

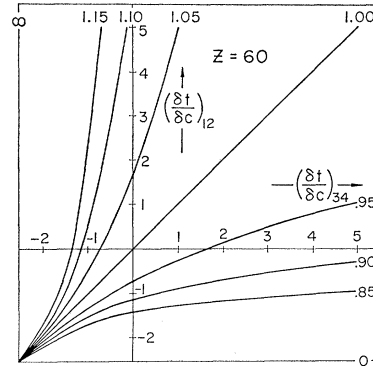


FIG. 1. Contours of constant value of the ratio \mathcal{R} of Eq. (16), plotted as a function of the two variables $\delta_{12} t / \delta_{12} c$ and $\delta_{34} t / \delta_{34} c$ for a Fermi distribution, $Z=60$. Each solid line is labeled with the corresponding value of \mathcal{R} .

have been observed. In such cases \mathcal{R} could deviate considerably from unity.

In Fig. 1, the ratio \mathcal{R} is plotted for $Z=60$, assuming a Fermi distribution. We conclude that \mathcal{R} will usually deviate from unity by less than 10%, except when the shifts are anomalously small.

If we tentatively identify the two ratios in Eq. (15), then the equation

$$[(\delta_{12} E)_{\text{opt}} - a_{12} C] / [(\delta_{34} E)_{\text{opt}} - a_{34} C] = (\delta_{12} E)_\mu / (\delta_{34} E)_\mu \quad (19)$$

can be solved for the specific-mass constant C . If shifts have been measured for several isotopes, as in Sn or Nd, then C can be obtained for any two pairs, and all should yield the same value. Any deviations could indicate that the muonic and optical ratios are not exactly equal. If the optical isotope shifts for the two pairs of isotopes are equal, however, then C is indeterminate.

A simple procedure is suggested by King.²² Neglecting the variation with isotopic mass of the specific-mass shift, we plot the muonic shifts (abscissa) versus the optical shifts (ordinate) of some particular optical line. The value at which the straight line that best fits all the points crosses the ordinate gives $(\delta E)_{\text{s.m.}}$. In this case, our assumption that the muonic and optical ratios can be equated is good to the extent that the points fall on a straight line. Note as well that deviations from a straight line could also imply that nuclear-polarization effects have not been properly taken into account.

III. EXPERIMENTAL PROCEDURE

A general discussion of the experimental techniques used in these measurements is given in the preceding paper.¹² We consider in this section only those modifications particular to the measurement of isotope shifts.

²² W. H. King, Proc. Roy. Soc. (London) **A280**, 430 (1964).

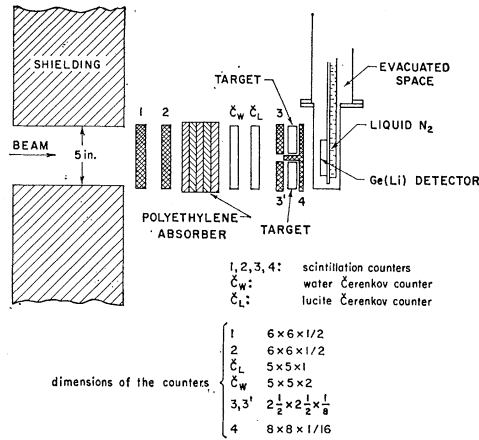


FIG. 2. Beam-telescope arrangement for running two targets simultaneously. Note the rib in the No. 4 counter which fits between the targets.

To achieve the maximum accuracy in the measurement of isotope shifts, it is desirable to minimize line shifts between spectra which originate from other than the isotopic variation itself. One possible technique to accomplish this is to measure two or more different isotopes simultaneously using the same Ge(Li) detector and electronics system. To differentiate between x rays originating from muons stopped in the different targets, identifying signals for each target are used to route the spectra to separate storage buffers in the computer. These signals are obtained by placing individual plastic scintillator counters (3 or 3') before each target, as shown schematically in Fig. 2. The signatures for a muon stopping in each target are $1234 \sim (\check{C}_L \text{ or } \check{C}_w)$ and $123'4 \sim (\check{C}_L \text{ or } \check{C}_w)$, where \sim means "not." The No. 4 counter (see Fig. 2) is designed with a rib that fits between the targets to eliminate events in which a muon enters a target, scatters into the other and stops there. When we used this technique in our measurements, experimental tests showed that leak through from one channel to the other was negligible. Any systematic differences between the data channels were determined and eliminated by alternating the position of the targets in consecutive runs.

Two other simpler techniques were also used to minimize the systematic errors in the isotope-shift measurements. One consists of running a composite target, made with one of the isotopes of proton number Z under study and a lower $Z' = (Z-2)$ or $(Z-3)$ element (e.g., $_{57}\text{La}$ with the Nd isotopes). Systematic errors are then determined and eliminated by checking the constancy of (a) the line width and the position of the lines of this reference target and (b) the gain in the region of interest, obtained from the full energy to double-escape separation of the K lines or the calibration spectrum, depending upon the energy region. The other technique, which can only be applied

to a very stable system, is to alternate isotopes and accumulate the spectra in corresponding separate storage buffers. The stability of the system can be checked by observing the constancy of the line widths.

All of the three techniques described above were used in our measurements of isotope shifts, and where different methods were applied to the same set of isotopes, the results were found to be in reasonable agreement.

The separated isotopes were obtained on loan from Oak Ridge National Laboratory. Their isotopic analysis and chemical forms are given in Table III. The material was packaged into thin aluminum containers, of dimensions $2\frac{1}{2}$ in. \times $2\frac{1}{2}$ in. and thickness determined by the quantity of isotope available. This meant that the target thickness varied from 0.5 g/cm^2 for the thinnest target to 2.5 g/cm^2 for most of the others.

IV. DATA ANALYSIS

The muonic and calibration spectra were stored on magnetic tape and plotted using a Calcomp recorder. Rough estimates of peak positions, widths, and heights obtained from the graphs provided a starting point for an iterative curve fitting routine.

The positions of the peaks were determined using a least-squares method by fitting either a Gaussian function (symmetric) or a Gaussian times a complementary error function (asymmetric) to the raw data. The background was fitted simultaneously with a polynomial function. The errors in the parameters of the functions used were obtained by finding the variation of each parameter that would increase the χ^2 by unity.

In order to ascertain whether systematic errors were introduced into our analysis by the procedure of fitting analytic functions to the data, we used two other methods to determine peak positions. One of these was to calculate the centroids of each peak, a method which is dependent upon the choice of background. We took care to take this into consideration, since the isotope shifts involving odd isotopes (with more complex line shapes) were determined principally in this manner. The errors quoted for isotope shifts involving odd isotopes are larger because of this factor. A second technique consisted of smoothing the data plot and differentiating it to determine the position of the maximum. All of these procedures gave results in reasonable agreement.

We used a simple procedure to correct for isotopic impurities. For a first approximation, the isotope shifts were determined without corrections from the muonic spectra. If muonic spectra were not available for all the isotopes, the additional isotope shifts were obtained from other sources, such as relative optical measurements. The muonic spectra were then refitted with a new function which included a line for each isotope that was present in the target in a significant amount. The relative intensities of the various lines

TABLE III. Isotopic composition of the nuclides studied.

Isotope	Isotopic composition							Sample number	Chemical form	Weight (g)
	40	42	43	44	46	48				
⁴⁰ Ca	99.87	0.07	<0.03	0.06	<0.03	<0.03		85501	CaCO ₃	250
⁴⁴ Ca	4.58	0.09	0.05	95.35	<0.02	<0.02		119001	CaCO ₃	214
	50	52	53	54						
⁵⁰ Cr	95.9	3.76	0.26	0.05				144901	Cr ₂ O ₃	57
⁵² Cr	0.02	99.74	0.23	0.01				83701	Cr ₂ O ₃	82
⁵³ Cr	<0.05	3.44	96.4	0.18				145101	Cr ₂ O ₃	140
⁵⁴ Cr	0.11	4.01	1.79	94.1				145201	Cr ₂ O ₃	29
	63	65								
⁶³ Cu	99.88	0.12						138902	Cu	104
⁶⁵ Cu	3.04	96.96						139090	Cu	37
	92	94	95	96	97	98	100			
⁹² Mo	97.6	0.74	0.46	0.34	0.15	0.44	0.29	134001	Mo	194
⁹⁶ Mo	0.28	0.58	96.8	1.54	0.36	0.45	<0.1	134201	Mo	202
⁹⁶ Mo	0.18	0.18	0.94	96.8	0.96	0.82	0.1	134301	Mo	197
⁹⁷ Mo	0.27	0.24	0.68	1.69	92.8	3.97	0.37	134401	Mo	95
	116	117	118	119	120	122				
¹¹⁶ Sn	95.74	1.02	1.49	0.32	1.06	0.13	0.15	126201	Sn	50
¹¹⁷ Sn	2.34	89.2	4.5	1.12	2.16	0.26	0.28	126301	Sn	29
¹¹⁸ Sn	0.39	0.4	97.15	0.64	1.2	0.1	0.12	126402	Sn	65
¹¹⁹ Sn	0.65	0.63	3.01	89.80	5.34	0.28	0.27	126501	Sn	71
¹²⁰ Sn	0.20	0.12	0.5	0.39	98.39	0.15	0.26	126601	Sn	82
¹²² Sn	1.01	0.58	1.91	0.77	3.75	90.8	1.16	126701	Sn	33
¹²⁴ Sn	0.92	0.49	1.60	0.58	2.36	0.77	93.28	126826	Sn	77
	142	143	144	145	146	148	150			
¹⁴² Nd	96.24	2.06	0.99	0.24	0.33	0.08	0.06	135101	Nd ₂ O ₃	173
¹⁴³ Nd	9.24	79.9	8.64	0.89	0.95	0.2	0.19	135201	Nd ₂ O ₃	34
¹⁴⁴ Nd	1.31	1.66	94.5	1.47	0.88	0.11	0.07	135301	Nd ₂ O ₃	189
¹⁴⁵ Nd	3.82	1.46	10.5	74.9	8.58	0.45	0.26	135401	Nd ₂ O ₃	24
¹⁴⁶ Nd	0.85	0.93	1.37	1.73	94.5	0.44	0.16	135501	Nd ₂ O ₃	154
¹⁴⁸ Nd	2.18	1.6	2.17	1.55	3.42	87.9	1.2	135601	Nd ₂ O ₃	64
¹⁵⁰ Nd	1.46	1.0	1.52	0.91	1.51	1.09	92.5	135701	Nd ₂ O ₃	46

TABLE IV. Muonic isotope shifts in Ca, Cr, Cu, and Mo. The field shifts are the observed shifts minus the reduced-mass shifts. The standard shifts are calculated for a uniform nuclear charge distribution with $R=1.2A^{1/3}$ fm.

Isotope pair	Observed shift (keV)	Field shift (keV)	Standard shift (keV)	$\delta E_{\text{field}}/(\delta E)_{\text{std}}$	
				This experiment	Other determinations
⁴⁰ Ca- ⁴⁴ Ca	0.99±0.10	1.19	3.26	0.36±0.04	0.33±0.02 ^a
⁵⁰ Cr- ⁵² Cr	-0.83±0.08	-0.73	2.60	-0.28±0.03	
⁵² Cr- ⁵³ Cr	0.70±0.08	0.75	1.27	0.59±0.06	
⁵² Cr- ⁵⁴ Cr	2.17±0.20	2.27	2.50	0.9±0.08	
⁶³ Cu- ⁶⁵ Cu	2.13±0.08	2.21	4.00	0.55±0.02	0.60±0.04 ^a
⁹² Mo- ⁹⁶ Mo	17.42±0.20	17.56	16.32	1.08±0.01	
⁹⁶ Mo- ⁹⁶ Mo	5.50±0.15	5.53	4.08	1.35±0.03	
⁹⁶ Mo- ⁹⁷ Mo	1.12±0.10	1.15	4.08	0.28±0.03	

^a Reference 8.

TABLE V. Muonic isotope shifts in Sn. The field shifts are the observed shifts corrected for the reduced-mass effect. The standard shifts are calculated for a uniform nuclear charge distribution with $R=1.2A^{1/3}$ fm.

Isotope pair	Observed shift (keV)	Field shift (keV)	Standard shift (keV)	$\delta E_{\text{field}}/\delta E_{\text{std}}$	
				This experiment	Other determinations
$^{116}\text{Sn}-^{117}\text{Sn}$	2.35 ± 0.10	2.38	5.15	0.46 ± 0.02	0.45 ± 0.03^a
$^{116}\text{Sn}-^{118}\text{Sn}$	6.10 ± 0.10	6.16	10.25	0.60 ± 0.01	0.630 ± 0.023
$^{118}\text{Sn}-^{119}\text{Sn}$	1.84 ± 0.16	1.87	5.10	0.37 ± 0.03	0.35 ± 0.04
$^{118}\text{Sn}-^{120}\text{Sn}$	5.23 ± 0.08	5.29	10.08	0.52 ± 0.01	0.521 ± 0.014
$^{120}\text{Sn}-^{122}\text{Sn}$	4.44 ± 0.15	4.49	9.93	0.45 ± 0.02	0.508 ± 0.016
$^{122}\text{Sn}-^{124}\text{Sn}$	4.39 ± 0.10	4.44	9.80	0.45 ± 0.01	
$^{116}\text{Sn}-^{124}\text{Sn}$	20.16 ± 0.20	20.38	40.06	0.503 ± 0.005	0.457 ± 0.015^b

^a Reference 8.

^b Reference 32.

were constrained to the known compositions (given in Table III), and the relative positions to the isotope-shift values obtained in the first approximation. After fitting this composite function, the isotope shifts were redetermined, and the procedure repeated with the new values until no change between initial and final values occurred. We found in all cases that only one application of this procedure was needed to account for the isotopic impurities.

To change the measured shifts from channel units to energy units we obtained the conversion factor, in some cases, from known γ -ray energies in the calibration spectrum, and in others, from full energy, single and double escape lines of the transition of interest. Typical values of this factor were from 0.396 keV/channel for Ca to 1.300 keV/channel for Nd. Since the isotope shifts are never more than 10 or 20 channels, it is not critical to know the conversion factor with high precision. Absolute energies were determined by doing a least-squares fit of a polynomial to the calibration spectrum, folding in the statistical errors in the data as well as the uncertainties in the standard values of the energy of the calibration lines.²³ The second-degree term in a quadratic fit, for example, was usually about 10^{-7} times the linear term.

In all isotopes except Nd, we determined only the isotope shifts in the $2p-1s$ transitions. For Nd, we also measured the shifts in the $3d-2p$ lines. The magnitude of these L shifts, however, is due mostly to dynamic hyperfine effects in the $2p$ levels (see Sec. II). Since the dynamic quadrupole interaction does not affect the $1s$ level and the effect on the $3d$ levels is negligible, dynamic quadrupole effects can be eliminated by adding the K and L shifts which involve the same $2p$ level (see Fig. 3). Moreover, since the isotope shift of the $3d$ levels is negligibly small, we have in this manner determined the isotope shift of the $1s$ level. Note that we obtain two values of $\delta(1s)$,

$$\delta(L\alpha_1) + (K\alpha_1) = \delta(1s),$$

$$\delta(L\alpha_2) + (K\alpha_2) = \delta(1s),$$

²³ See Table III, preceding paper.

which must be equal. This procedure also provides us with a check on the internal consistency of our measurements.

V. RESULTS AND DISCUSSION

The results of our measurements of muonic isotope shifts are given in Tables IV–VII. The shifts in Ca, Cr, Cu, and Mo appear in Table IV, while the Sn shifts appear in Table V. The Nd K - and L -line isotope shifts are given in Table VI; the $1s$ level shifts, in Table VII. In Tables IV, V, and VII, we have included standard isotope shifts and the ratio

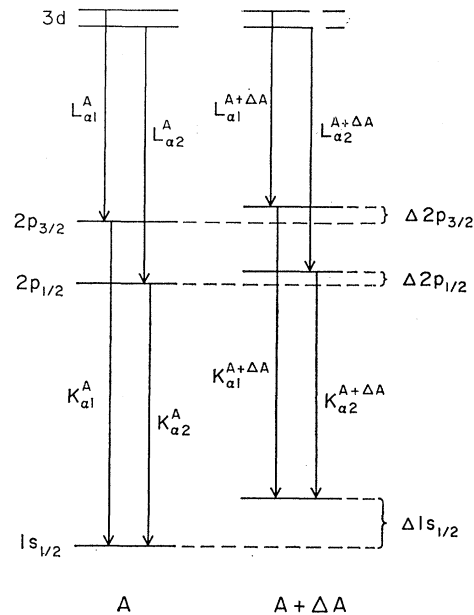


FIG. 3. Lowest muonic levels for two isotopes differing by ΔA neutrons. The $3d$ levels are assumed to have equal binding energy in the two isotopes. It is apparent, for example, that

$$\delta(1s) = (L_{\alpha_1}^A + K_{\alpha_1}^A) - (L_{\alpha_1}^{A+\Delta A} + K_{\alpha_1}^{A+\Delta A}),$$

and so on, where, for example, $L_{\alpha_1}^A$ is the L_{α_1} energy for mass number A .

TABLE VI. Muonic isotope shifts of the K and L lines of the Nd isotopes. The use of the subscripts can be understood from Fig. 3.

Isotopes	δK_{α_1} (keV)	δK_{α_2} (keV)	δL_{α_1} (keV)	δL_{α_2} (keV)
^{142}Nd - ^{144}Nd	15.68 ± 0.15	15.56 ± 0.15	0.38 ± 0.10	0.50 ± 0.10
^{144}Nd - ^{146}Nd	15.20 ± 0.15	14.38 ± 0.15	0.01 ± 0.10	0.83 ± 0.10
^{146}Nd - ^{148}Nd	17.72 ± 0.15	16.74 ± 0.15	-0.96 ± 0.10	0.02 ± 0.10
^{148}Nd - ^{150}Nd	37.09 ± 0.15	25.46 ± 0.15	-15.54 ± 0.10	-3.91 ± 0.10

TABLE VII. Muonic isotope shifts of the $1s$ level in the Nd isotopes. The nuclear-polarization corrections are from Ref. 14. The field shifts are the observed shifts corrected for reduced-mass effects and nuclear-polarization effects. The standard shifts are calculated for a uniform nuclear charge distribution with $R=1.2A^{1/3}$ fm.

Isotope pair	Observed shift (keV)	Nuclear-polarization correction (keV)	Field shift (keV)	Standard shift (keV)	$\delta E_{\text{field}}/\delta E_{\text{std}}$
^{142}Nd - ^{148}Nd	6.03 ± 0.30		6.05	6.70	0.90 ± 0.06
^{144}Nd - ^{146}Nd	5.78 ± 0.50		5.80	6.61	0.88 ± 0.09
^{142}Nd - ^{144}Nd	16.06 ± 0.20	0.19	16.30	13.37	1.22 ± 0.01
^{144}Nd - ^{146}Nd	15.21 ± 0.20	0.32	15.58	13.20	1.18 ± 0.01
^{146}Nd - ^{148}Nd	16.76 ± 0.20	0.64	17.44	13.05	1.34 ± 0.01
^{148}Nd - ^{150}Nd	21.55 ± 0.25	1.50	23.08	12.92	1.79 ± 0.02

TABLE VIII. Values of the odd-even staggering parameter γ_N [defined by Eq. (20)]. The muonic Mo values were obtained by using muonic results and relative optical isotope shifts corrected for specific-mass effects, as explained in Sec. VD. The optical values for Mo and Nd have been corrected for specific-mass shifts using our results, the Sn values using those of Ref. 32. (See text.) The optical data are from Refs. 29 and 30 for Mo, Refs. 31 and 38 for Sn, and Ref. 39 for Nd. The electronic x-ray data are from Ref. 40.

Isotope	This experiment	γ_N Optical	Electronic x ray
^{53}Cr	0.70 ± 0.08	(6032 Å)	(5793 Å)
^{96}Mo	0.64 ± 0.15	0.58 ± 0.10	0.69 ± 0.10
^{97}Mo	0.34 ± 0.08	0.40 ± 0.07	0.31 ± 0.07
^{117}Sn	0.77 ± 0.05	0.73 ± 0.10	
^{118}Sn	0.70 ± 0.08	0.59 ± 0.10	
		(5621 Å)	(4845 Å)
^{148}Nd	0.75 ± 0.08	0.93 ± 0.12	0.60 ± 0.08
^{146}Nd	0.76 ± 0.12	0.84 ± 0.11	0.23 ± 0.18

TABLE IX. Fine-structure splittings of the muonic K and L lines in the Nd isotopes. The corrected values are the measured values with dynamic quadrupole interaction effects subtracted. The values of these corrections are listed in Table I.

	$K_{f.s.}$ (in keV)		$L_{f.s.}$ (in keV)	
	Measured	Corrected	Measured	Corrected
^{142}Nd	81.62 ± 0.20	81.63	69.35 ± 0.15	69.36
^{144}Nd	81.50 ± 0.20	81.55	69.23 ± 0.15	69.28
^{146}Nd	80.68 ± 0.20	80.91	68.41 ± 0.15	68.64
^{148}Nd	79.70 ± 0.20	80.52	67.43 ± 0.15	68.29
^{150}Nd	68.07 ± 0.20	79.36	55.80 ± 0.15	67.09

TABLE X. Measured K and L transition energies and derived values of the parameters of the nuclear charge distributions of the Nd isotopes. The Fermi distribution is given by Eq. (5), the deformed Fermi distribution by Eq. (6). The values of the parameter β are from Refs. 16 and 17.

Isotope	Line	Measured energy (keV)	Fermi distribution		Deformed Fermi distribution		
			c (fm)	t (fm)	c (fm)	t (fm)	β
^{142}Nd	$K\alpha_1$	4352.06 ± 0.40	5.75 ± 0.03	2.38 ± 0.08	5.80 ± 0.03	2.32 ± 0.08	0.104
	$K\alpha_2$	4270.44 ± 0.50					
	$L\alpha_1$	1402.97 ± 0.25					
	$L\alpha_2$	1472.32 ± 0.25					
^{144}Nd	$K\alpha_1$	4336.38 ± 0.45	5.80 ± 0.03	2.37 ± 0.08	5.85 ± 0.03	2.27 ± 0.08	0.123
	$K\alpha_2$	4254.88 ± 0.55					
	$L\alpha_1$	1402.59 ± 0.25					
	$L\alpha_2$	1471.82 ± 0.25					
^{146}Nd	$K\alpha_1$	4321.18 ± 0.40	5.77 ± 0.03	2.45 ± 0.08	5.82 ± 0.03	2.42 ± 0.08	0.151
	$K\alpha_2$	4240.50 ± 0.50					
	$L\alpha_1$	1402.58 ± 0.20					
	$L\alpha_2$	1470.99 ± 0.25					
^{148}Nd	$K\alpha_1$	4303.46 ± 0.45	5.80 ± 0.03	2.46 ± 0.08	5.84 ± 0.03	2.40 ± 0.08	0.197
	$K\alpha_2$	4223.76 ± 0.50					
	$L\alpha_1$	1403.54 ± 0.25					
	$L\alpha_2$	1470.97 ± 0.25					
^{150}Nd	$K\alpha_1$	4266.37 ± 0.40	5.90 ± 0.03	2.42 ± 0.08	5.86 ± 0.03	2.35 ± 0.08	0.279
	$K\alpha_2$	4198.30 ± 0.50					
	$L\alpha_1$	1419.08 ± 0.25					
	$L\alpha_2$	1474.88 ± 0.25					

of the measured to the standard shifts. It should be noted that the standard field-effect shifts have been calculated exactly to all orders by solving the Dirac equation numerically for the muon in the field of the extended nuclear charge distribution.

The odd-even staggering parameter γ_N is defined as

$$\gamma_N = \delta E(N-1, N) / \frac{1}{2} \delta E(N-1, N+1), \quad (20)$$

where N is the neutron number of the odd- A isotope. We have determined the values of γ_N for the odd- N nuclei that we studied; they are given in Table VIII.

The measured fine-structure splittings of the K and

L lines in the Nd isotopes are presented in Table IX. In Table X, we present the values of c and t for two distributions for the same isotopes, as determined by our analysis for the measured K and L energies.

The specific-mass shifts determined in the comparison of muonic and optical isotope shifts are given in Tables XI–XIII for Cr, Mo, and Nd, respectively. A comparison of muonic, optical, and electronic x-ray results for the ratio $(\delta E)_{\text{field}} / (\delta E)_{\text{std}}$ in the Nd isotopes appears in Table XIV.

In the following, we discuss separately the results for each element.

TABLE XI. Specific-mass shifts in three optical lines of chromium determined by comparison with muonic results. The optical data are from Ref. 27 ($1 \text{ mK} = 10^{-3} \text{ cm}^{-1}$).

λ (Å)	Isotope pair	Measured shift (mK)	Reduced-mass shift (mK)	Specific-mass shift (mK)	Corrected shift (mK)
4254	^{50}Cr - ^{52}Cr	-4.4 ± 0.2	-9.9	6.4 ± 0.6	-0.9
	^{52}Cr - ^{54}Cr	0.0 ± 0.2	-9.2	6.4 ± 0.6	2.8
4274	^{50}Cr - ^{52}Cr	-4.0 ± 0.1	-9.9	6.8 ± 0.5	-0.9
	^{52}Cr - ^{54}Cr	0.5 ± 0.2	-9.2	6.8 ± 0.6	2.9
4289	^{50}Cr - ^{52}Cr	-3.6 ± 0.3	-9.9	7.2 ± 0.8	-0.9
	^{52}Cr - ^{54}Cr	0.7 ± 0.2	-9.2	7.2 ± 0.7	2.7

TABLE XII. Specific-mass shifts in two lines of molybdenum determined by comparison with muonic results. The optical data are from Ref. 29 for the 5793-Å line and from Ref. 30 for the 6032-Å line.

λ (Å)	Isotope pair	Measured shift (mK)	Reduced-mass shift (mK)	Specific-mass shift (mK)	Corrected shift (mK)	Relative shift
5793	^{92}Mo - ^{94}Mo	24.0 ± 1.4	-2.0	-18.6 ± 1.5	44.6 ± 2.0	1.00 ± 0.05
	^{94}Mo - ^{96}Mo	17.6 ± 1.4	-2.0	-18.6 ± 1.5	38.3 ± 2.0	0.86 ± 0.06
	^{96}Mo - ^{98}Mo	10.8 ± 1.4	-2.0	-18.6 ± 1.5	31.4 ± 2.0	0.70 ± 0.06
	^{98}Mo - ^{100}Mo	25.5 ± 1.4	-2.0	-18.6 ± 1.5	46.1 ± 2.0	1.03 ± 0.08
	^{95}Mo - ^{96}Mo	14.7 ± 1.4	-1.0	-9.3 ± 0.8	25.0 ± 1.8	
	^{96}Mo - ^{97}Mo	-5.5 ± 1.4	-1.0	-9.3 ± 0.8	4.8 ± 1.8	
6032	^{92}Mo - ^{94}Mo	21.3 ± 3.0	-1.9	-32.6 ± 3.2	55.8 ± 4.5	1.00 ± 0.07
	^{94}Mo - ^{96}Mo	24.2 ± 3.0	-1.9	-32.6 ± 3.2	55.8 ± 4.5	1.05 ± 0.11
	^{96}Mo - ^{98}Mo	7.8 ± 3.0	-1.9	-32.6 ± 3.2	42.3 ± 4.5	0.76 ± 0.08
	^{98}Mo - ^{100}Mo	25.0 ± 2.0	-1.9	-32.6 ± 3.2	59.5 ± 3.8	1.07 ± 0.11
	^{95}Mo - ^{96}Mo	22.4 ± 2.0	-1.0	-16.3 ± 1.6	39.7 ± 3.1	
	^{96}Mo - ^{97}Mo	-8.9 ± 2.0	-1.0	-16.3 ± 1.6	8.4 ± 3.1	

TABLE XIII. Specific-mass shifts and the specific-mass constants of various optical lines determined by comparison with muonic results for the ^{142}Nd - ^{144}Nd isotope pair. The optical data for the 5621- and 4945-Å lines are from Ref. 39; for the rest of the lines, from Ref. 41.

λ (Å)	Isotope pair	Measured shift (mK)	Reduced-mass shift (mK)	Specific-mass constant (units of 10^4 mK)	Specific-mass shift (mK)	Corrected shift (mK)
5621	^{142}Nd - ^{144}Nd	21.23 ± 0.30	-0.95	-17.6 ± 1.8	-17.2 ± 1.7	39.4 ± 1.8
4945		-20.85 ± 0.30	-1.08	-13.1 ± 1.7	-12.8 ± 1.7	-7.0 ± 1.8
5675		20.4 ± 0.4	-0.94	-20.4 ± 2.1	-20.0 ± 2.1	41.3 ± 2.2
5291		-74.1 ± 0.5	-1.01	2.0 ± 5.2	2.0 ± 5.2	-75.1 ± 5.4
4924		-32.4 ± 0.4	-1.08	-8.0 ± 2.7	-7.9 ± 2.5	-23.4 ± 2.5
4688		-100.9 ± 1	-1.14	7.2 ± 8.4	7.1 ± 8.2	106.9 ± 8.3
5293		41.6 ± 0.6	-1.01	-28.2 ± 3.7	-27.6 ± 3.3	20.2 ± 3.4
5319		38.0 ± 0.8	-1.00	-13.2 ± 3.9	-12.9 ± 3.7	51.9 ± 3.8
5273		50.6 ± 0.6	-1.01	-15.3 ± 4.0	-15.0 ± 3.9	66.6 ± 4.0
4061		-47.9 ± 0.6	-1.31	-6.7 ± 3.8	-6.6 ± 3.7	-40.0 ± 3.8

TABLE XIV. Comparison of the values of $(\delta E)_{\text{field}}/(\delta E)_{\text{std}}$ and of the relative isotope shifts for the Nd isotopes obtained from the present muonic work, the optical results of Gerstenkorn *et al.* (Ref. 14) and the electronic x-ray measurements of Bhattacharjee *et al.* (Ref. 40). The optical value of $(\delta E)_{\text{std}}$ is quoted in Ref. 41.

Isotope pair	$(\delta E)_{\text{field}}/(\delta E)_{\text{std}}$			Relative shifts		
	Muonic	Optical ^a	Electronic x rays	Muonic	Optical ^a	Electronic x rays
^{142}Nd - ^{144}Nd	1.22 ± 0.01	1.21 ± 0.06	1.39 ± 0.07	1.00 ± 0.01	1.00 ± 0.05	1.00 ± 0.06
^{144}Nd - ^{146}Nd	1.18 ± 0.01	1.16 ± 0.05	1.10 ± 0.15	0.96 ± 0.01	0.95 ± 0.05	0.79 ± 0.11
^{146}Nd - ^{148}Nd	1.34 ± 0.01	1.24 ± 0.06	1.30 ± 0.16	1.07 ± 0.01	1.02 ± 0.05	0.93 ± 0.12
^{148}Nd - ^{150}Nd	1.79 ± 0.02	1.72 ± 0.06	1.91 ± 0.10	1.42 ± 0.02	1.41 ± 0.05	1.37 ± 0.07

^a For 5675-Å line (Ref. 41) with specific-mass corrections given in Table XIII, and $(\delta E)_{\text{std}} = 34$ mK.

A. Calcium

The charge distributions and the isotope shifts between the Ca isotopes have been extensively studied by both electron scattering and muonic x-ray techniques. ^{40}Ca and ^{48}Ca are both doubly magic nuclei, which makes the study of the change of the nuclear charge distribution in the Ca isotopes particularly interesting. The isotopes shift between ^{40}Ca and ^{44}Ca was found to be surprisingly small in 1963 by using a NaI technique in muonic measurements.² This was soon confirmed by electron scattering measurements²⁴ which revealed, in addition, the detailed variation of the charge distribution, particularly, the decrease of the skin thickness in the heavier isotopes. Recently, the muonic isotope shifts of several pairs (40–42, 40–44, and 40–48) have been investigated (with greater precision) by Ehrlich *et al.*²⁵ A detailed comparison between muonic and electron scattering results on the Ca isotope can be found in Ref. 8. We have also measured the isotope shift between ^{40}Ca – ^{44}Ca . The result listed in Table IV is in good agreement with Ehrlich's.

The muonic isotope shifts in Ca together with the electron scattering results indicate that the skin thickness changes by up to several percent from one isotope to another. It should be borne in mind that this observation may be more a characteristic of the Ca isotopes than a general behavior among the isotopes of all elements. As we will show later, in our studies of the Nd isotopes, where both *K* and *L* x rays were measured, the skin thickness of the even Nd isotopes was found to be nearly constant within the experimental uncertainties among the isotopes. For the tin isotopes, Ehrlich⁸ has concluded that among the even isotopes, the change in *t* never exceeds 3% of its mean value if exact agreement with optical results is required. Recently, Schiffer *et al.*²⁶ have analyzed Coulomb energies from studies of analog states to obtain information regarding nuclear radii. They found that the behavior of the charge radius among the Ca isotopes is quite different from that among Ni and Sn isotopes (which also have a magic number of protons, at 28 and 50). The rms charge radii for the Ca isotopes remains relatively constant from ^{42}Ca to ^{45}Ca and then drops off rapidly from ^{46}Ca on, while the charge radii of Ni and Sn isotopes increase monotonically with *A*, though at a rate somewhat slower than $A^{1/3}$.

B. Chromium

It is known from optical-isotope-shift measurements that, in the neighborhood of closed neutron shells, the

²⁴ R. Hofstadter, G. K. Noldecke, K. J. Van Ostrum, L. R. Suelzle, M. R. Yearian, B. C. Clark, R. Herman, and D. G. Ravenhall, *Phys. Rev. Letters* **15**, 758 (1965).

²⁵ R. D. Ehrlich, D. Fryberger, D. A. Jensen, C. Nissim-Sabat, R. J. Powers, V. L. Telegdi, and C. K. Hargrove, *Phys. Rev. Letters* **18**, 959 (1967); **19**, 334 (1967).

²⁶ J. P. Schiffer, J. A. Nolen, Jr., and N. Williams, *Phys. Letters* **29B**, 399 (1969).

nuclear charge radius varies irregularly with the neutron number. Specifically, optical results have shown that the addition of two neutrons to complete the neutron shells at $N=50$, 82, and 126 changes the nuclear charge radius far less than the further addition of two neutrons.¹ The neutron number of the stable chromium isotopes varies from 26 to 30, including the closed shell at 28. Chromium should therefore be a good example of such closed-shell effects.

The measured muonic isotope shifts in Cr are given in Table IV. The negative experimental shift between ^{50}Cr and ^{52}Cr indicates that the nuclear charge radius decreases from the lighter to the heavier isotope. This could be partially due to the decrease in deformation from ^{50}Cr to ^{52}Cr [$\beta(50)=0.31$, $\beta(52)=0.23$].¹⁶ The standard volume shift is 2.60 keV; the deformation effect would reduce this value to 0.9 keV. We could therefore explain the experimental result of -0.8 keV as due to the large decrease in β deformation accompanied by an unusually small increase in volume, caused by the closing of the neutron shell at $N=28$.

Between ^{52}Cr and ^{54}Cr , the deformation increases [$\beta(54)=0.27$], accounting for part of the positive shift which we have observed for this pair of isotopes. The observed value, however, is considerably smaller than expected for an incompressible deformed nuclear charge distribution.

The shift between ^{52}Cr and ^{53}Cr is smaller than half the 52–54 shift, an example of odd-even staggering (see Table VIII).

Since mass effects are much larger than field effects in light nuclei, optical-isotope-shift measurements are not usually made for elements with $Z \leq 40$. The closing of the $N=28$ shell in ^{52}Cr , however, makes the chromium isotopes particularly interesting. A measurement of the ^{50}Cr – ^{52}Cr and ^{52}Cr – ^{54}Cr optical shifts has been recently made by Heiling and Wendlandt.²⁷ Their results are summarized in Table XI, in which we have also included the estimated values of the reduced-mass corrections. We have determined, by comparison with our muonic data, the values of the specific-mass shifts in each of these lines. These are also given in Table XI. We note that the specific-mass shifts are of the same order of magnitude as the reduced-mass shifts, but of opposite sign. Moreover, as expected for such low *Z*, the field-effect shift is much smaller than the mass-effect shifts, which emphasizes the difficulty in the interpretation of optical measurements for light nuclei.

C. Copper

The isotope shift between the odd copper isotopes is given in Table IV. Our value, about half the standard value is in good agreement with a previous muonic measurement.⁸

²⁷ K. Heilig and D. Wendlandt, *Phys. Letters* **25A**, 277 (1967).

D. Molybdenum

We have studied the muonic spectra of two even and two odd isotopes of Mo. The isotope shifts are given in Table IV.

The measured ^{92}Mo - ^{96}Mo shift is larger than the standard value. If the change in deformation is taken into account, however, the standard shift increases to ~ 20.4 keV, which indicates that the measured value is smaller than the "incompressible" value.

In order to evaluate the odd-even staggering parameter for the odd isotopes, we need some supplementary information. There is in the literature a report of an earlier measurement of the muonic isotope shift between ^{96}Mo and ^{98}Mo ,²⁸ but no measurement of the muonic shift between ^{94}Mo and ^{96}Mo . We have therefore obtained these shifts by using accurate relative isotope shifts from optical measurements, corrected for specific-mass effects as follows.

The optical isotope shifts in Mo have been measured in various transitions. In only two cases, however, have even-odd shifts been included. Because our muonic results consist only of the ^{92}Mo - ^{96}Mo , ^{95}Mo - ^{96}Mo , and ^{96}Mo - ^{97}Mo shifts, we can only compare them with these. The results of Hughes²⁹ for the line at 5793 Å and those of Arroe and Cornwall³⁰ for the line at 6032 Å are summarized in Table XII.

We have obtained the specific-mass shifts in these optical lines from the plot of relative muonic shifts versus optical shifts in Fig. 4. It should be noted that we have plotted shifts per neutron; therefore, the specific-mass shift obtained from the figure is correspondingly *per neutron*. The points in this plot fit a straight line reasonably well, within the quoted error

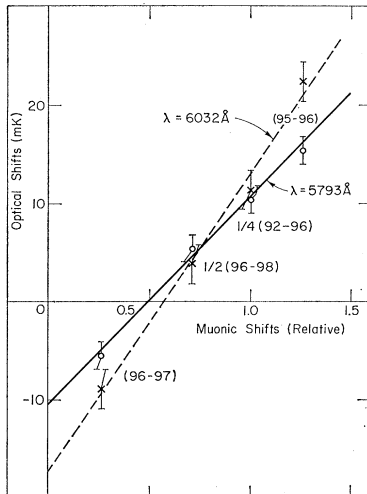


FIG. 4. Plot of optical isotope shifts versus relative muonic isotope shifts in Mo. The shifts are for a 1-neutron difference. The optical data is from Refs. 29 and 30.

²⁸ C. Chasman, R. A. Ristinen, R. C. Cohen, S. Devons, and C. Nissim-Sabat, Phys. Rev. Letters **14**, 181 (1965).

²⁹ R. H. Hughes, Phys. Rev. **121**, 499 (1961).

³⁰ H. Arroe and J. M. Cornwall, Phys. Rev. **117**, 748 (1960).

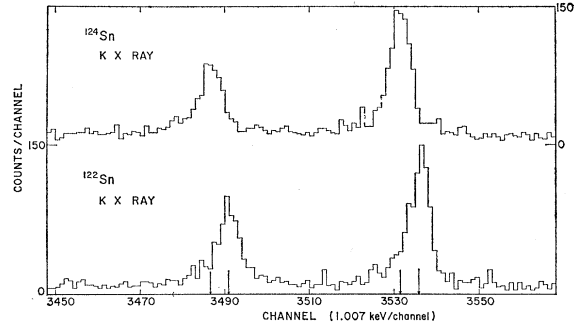


FIG. 5. Muonic K x-ray spectrum of ^{122}Sn and ^{124}Sn . The gain is 1.007 keV/channel. The arrows at the bottom of the figure indicate the position of the peaks. The separation is slightly more than four channels.

bars, showing the validity of our assumptions, as discussed in Sec. II C. The reduced- and specific-mass shifts are quoted in Table XII. We have included in Fig. 4 the ^{96}Mo - ^{98}Mo muonic shift.²⁸

We note, from the results given in Table XII, that the observed negative optical shift between ^{96}Mo and ^{97}Mo is a consequence of the large value of the specific-mass shifts. In the last column of this table the relative values are given of the corrected shifts between even isotopes. Note also that the relative 94–96 shifts have somewhat different values for the two transitions. In order to calculate the odd-even staggering parameters, we have derived the muonic 94–96 and 96–98 isotopes shifts from our measurement of the 92–96 shift and from an average of the relative optical values for the two lines. These are

$$\Delta E(^{94}\text{Mo}-^{96}\text{Mo}) = 8.1 \pm 0.8 \text{ keV,}$$

$$\Delta E(^{96}\text{Mo}-^{98}\text{Mo}) = 6.6 \pm 0.6 \text{ keV.}$$

The value for the muonic ^{96}Mo - ^{98}Mo shift obtained by Chasman *et al.*²⁸ is 6.2 ± 0.7 keV, in good agreement with the value determined above. The odd-even staggering parameters calculated with these values are given in Table VIII.

E. Tin

The isotope shifts among seven muonic tin isotopes (116, 117, 118, 119, 120, 122, 124) were investigated; the observed shifts, the evaluated field-effect shifts and the ratios of $(\delta E)_{\text{field}}/(\delta E)_{\text{std}}$ are listed in Table V. The odd-even staggering parameters are given in Table VIII. Ehrlich's⁸ recent results are also listed in Table V for comparison purposes. The isotope shifts studied by both groups (116–117, 116–118, 118–119, 118–120, 120–122) are in good agreement except that for the pair (120–122), for which a difference in the shifts of 0.5 ± 0.23 keV is observed. The (122–124) shift was not measured by Ehrlich. The K x-ray spectra for the two isotopes ^{122}Sn and ^{124}Sn are shown in Fig. 5.

Several measurements of optical isotope shifts of tin

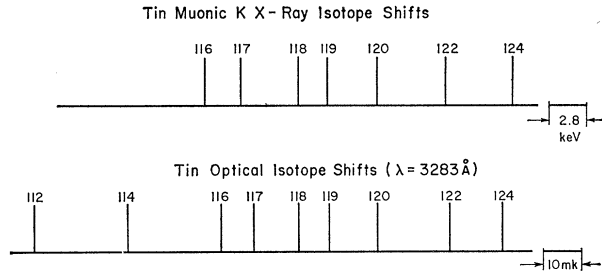


FIG. 6. Relative muonic and optical isotope shifts in Sn. The scale is at the right on the figure. The optical data are from Ref. 31.

have been made, the most precise and extensive by Stacey.³¹ The relative muonic and optical shifts are compared schematically in Fig. 6. The electron x-ray isotope shift of tin has been reported only for the pair ^{116}Sn – ^{124}Sn .³² To obtain the field effects in the optical results, the specific-mass correction must be first extracted. By using the method of King,²² Stacey was able to put a limit on the value of the specific-mass correction of not less than 4 mK ($1 \text{ mK} = 10^{-3} \text{ cm}^{-1}$). By comparing the optical and electronic x-ray results between the pair (116–124), a value to $-3.13 \pm 0.25 \text{ mK}$ was obtained.³² By directly comparing the optical and muonic x-ray results of even isotopes of tin, Ehrlich⁸ obtained a value of $-3.3 \pm 0.6 \text{ mK}$ which is in agreement with the other results quoted above. In this type of extraction of the specific-mass correction in optical shifts by normalizing to the muonic isotope shifts, the effect of the higher moments of the nuclear charge distribution is negligible because only the ratios of the shifts enter into the normalization. As shown in Sec. II C, when variations of the skin thickness (δt) are only a few percent, the ratios of energy shifts are approximately equal to the ratios of the variations of the second moments $\delta \langle r^2 \rangle$. However, in a careful examination, the variations of the muonic isotope shifts in even tin isotopes are seen not to be in close agreement with the optical shifts, as shown in Fig. 7. Particularly, our measurement of the isotope shift between ^{122}Sn and ^{124}Sn showed a marked deviation from the optical shift (see Fig. 7). In the optical results, after the specific-mass correction (-3 mK) is made, the shift between ^{122}Sn and ^{124}Sn is less than 60% of the shift between ^{120}Sn and ^{122}Sn . In our muonic results, these two shifts are both equal to 4.5 keV. Figure 5 is a direct comparison of the K lines of ^{122}Sn and ^{124}Sn ; a shift of 4.5 keV is clearly evident.

There are two possible ways to explain this discrepancy. One is that the optical or muonic measurements of ^{122}Sn – ^{124}Sn are in error. In view of the agreement between our results and Ehrlich's in five pairs of the Sn isotopes, the error in the shift in ^{122}Sn – ^{124}Sn

would be expected to be no more than $\pm 0.6 \text{ keV}$. Moreover, Hindmarsh and Kuhn,³³ in an earlier and considerably less precise measurement in a different optical line, found the 120–122 and 122–124 shifts to be equal. The other explanation is that the nuclear configurations undergo an abrupt change from ^{122}Sn to ^{124}Sn , which is somehow manifested by a sudden drop in the optical isotope shift but not in the muonic results. This is possible, but it is hard to understand. The even tin isotopes are very similar. The nuclei are spherical, with low-energy level schemes that are very much alike and change smoothly from ^{116}Sn to ^{124}Sn . This is also evident in the prediction of several theoretical calculations of the optical isotope shifts based upon different nuclear models. Uher and Sorensen,³⁴ using the pairing plus quadrupole model, have predicted a value of $\delta E / (\delta E)_{\text{std}} \sim 0.5$ for all isotope pairs. In a calculation based on the theory of finite Fermi systems, Krainov and Mikulinskii³⁵ found a value of $\delta E / (\delta E)_{\text{std}} \sim 0.89$ for the (116–118) and (118–120) pairs and a value equal to 0.61 for the (120–122) and (122–124) pairs. (We have used calculated values of $(\delta E)_{\text{std}}$ of Babushkin³⁶ in order to obtain the quoted values of this ratio.) The results of a similar calculation by Bunatyan³⁷ are listed below [also obtained with $(\delta E)_{\text{std}}$ values from Ref. 36].

Isotope pair	$(\delta E) / (\delta E)_{\text{std}}$
(116–118)	0.49
(118–120)	0.41
(120–122)	0.33
(122–124)	0.26

[It should be noted that Krainov and Mikulinskii assume that the extra neutron pairs between ^{118}Sn and ^{116}Sn and between ^{120}Sn and ^{118}Sn are $(1g_{7/2})^2$ pairs, whereas the extra neutron pairs between ^{122}Sn and ^{120}Sn and between ^{124}Sn and ^{122}Sn are $(1h_{11/2})^2$ pairs. Bunatyan, on the other hand, takes all these neutron pairs as $(1h_{11/2})^2$ pairs.]

None of these three calculations would explain a sudden drop in the optical isotope shift for ^{122}Sn – ^{124}Sn . The variation of the observed muonic isotope shifts in tin is in quite good agreement with the theoretical predictions, as shown in Fig. 7.

An attempt was made to extract the specific-mass correction by normalizing the even optical isotope shifts with the corresponding muonic results. However, because of the poor agreement, no satisfactory straight line can be drawn through all the points that still gives a reasonable value for the specific-mass correction.

³³ W. H. Hindmarsh and H. G. Kuhn, Proc. Phys. Soc. (London) **68A**, 433 (1955).

³⁴ R. A. Uher and R. A. Sorensen, Nucl. Phys. **86**, 1 (1966).

³⁵ V. P. Krainov and M. A. Mikulinskii, Yadern Fiz. **4**, 928 (1967) [English transl.: Soviet J. Nucl. Phys. **4**, 665 (1967)].

³⁶ F. A. Babushkin, Zh. Eksperim. i Teor. Fiz. **44**, 1661 (1963) [English transl.: Soviet Phys.—JETP **17**, 1118 (1963)].

³⁷ G. G. Bunatyan, Yadern Fiz. **4**, 707 (1967) [English transl.: Soviet J. Nucl. Phys. **4**, 502 (1967)].

³¹ D. N. Stacey, Proc. Roy. Soc. (London) **A280**, 439 (1964).

³² R. B. Chesler and F. Boehm, Phys. Rev. **166**, 1206 (1968).

Isotope Shifts in Even $_{50}\text{Sn}$ Isotopes

FIG. 7. (a) Plot of optical isotope shifts (I.S.) versus relative muonic shifts in Sn. The optical data are from Ref. 31. It is obvious that the points do not lie on a straight line, especially the (122-124) shift. Note that we are plotting shifts per *two*-neutron difference. (b) Plot of measured and calculated relative isotope shifts in Sn. Note that the muonic results follow a trend which is similar to those of the calculations. The measured optical results are from Ref. 31; the calculated values, from Refs. 34 and 37.

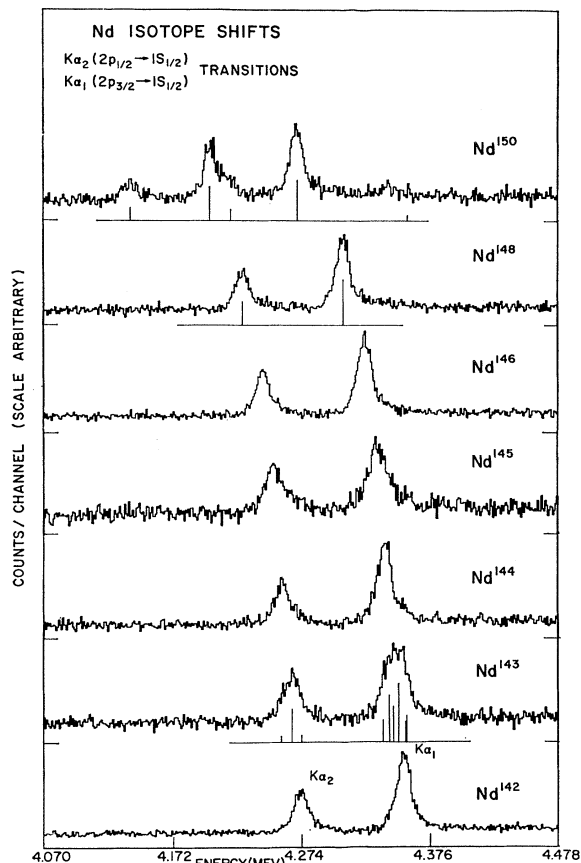
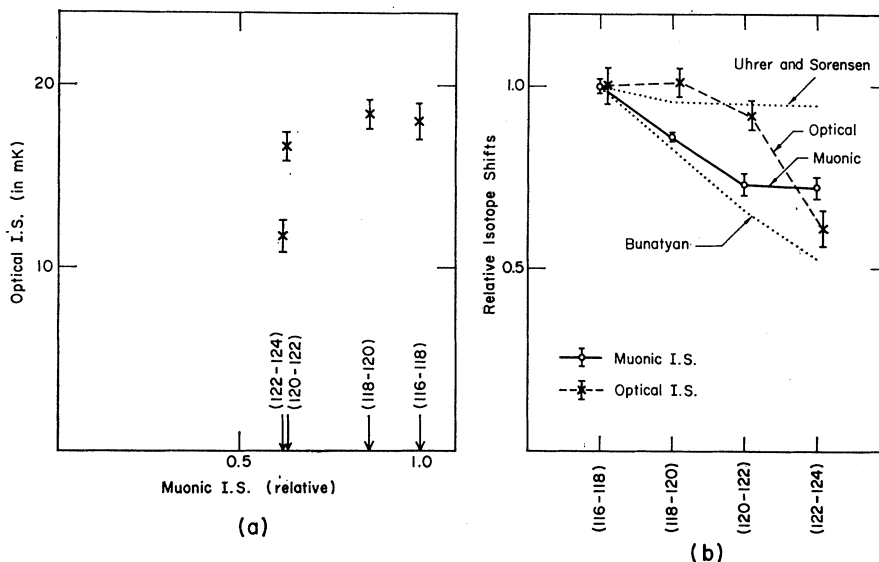


FIG. 8. Muonic K x-ray spectra of seven Nd isotopes. Note the broadening of the lines of the odd isotopes and the more complex spectrum of ^{150}Nd . Below the ^{143}Nd peaks are shown the four static-quadrupole-splitting components for the $K\alpha_1$ line and two components due to isotopic impurities for both lines. Below the ^{150}Nd spectrum are shown the principal dynamic-quadrupole-splitting components.

Stacey's group has recently remeasured the even-odd shifts³⁸; from these later values one obtains the odd-even staggering parameters

$$\gamma_{117} = 0.73 \pm 0.10,$$

$$\gamma_{119} = 0.59 \pm 0.10.$$

The first value is in good agreement with our muonic results (see Table VIII), but γ_{119} is somewhat larger than our value, though within the error.

F. Neodymium

It is well established that the optical isotope shifts for pairs of isotopes with 88 and 90 neutrons in $_{60}\text{Nd}$, $_{62}\text{Sm}$, and $_{63}\text{Eu}$ are anomalously large.¹ This is directly related to a change of the neutron-shell configuration. According to the Nilsson nuclear model, the sudden onset of permanent deformation occurs at a neutron number of 90. The increase in the deformation is reflected by the unusually large values of (δE) (deformation), and hence of the total measured isotope shifts.

To explore the variation of the nuclear charge distribution in this interesting transition region, we have made precise measurements of the energies and isotope shifts of the muonic K and L lines in the Nd isotopes (142, 143, 144, 145, 146, 148, and 150). Because the deformation increases with neutron number for these isotopes, the volume-effect shift is reinforced by the deformation-effect shift (i.e., the observed isotope shifts are larger than the standard). These large shifts (of the order of tens of keV) can be seen clearly in Fig. 8.

The structure of the $K\alpha_1$ lines of the odd isotopes

³⁸ D. N. Stacey (private communication).

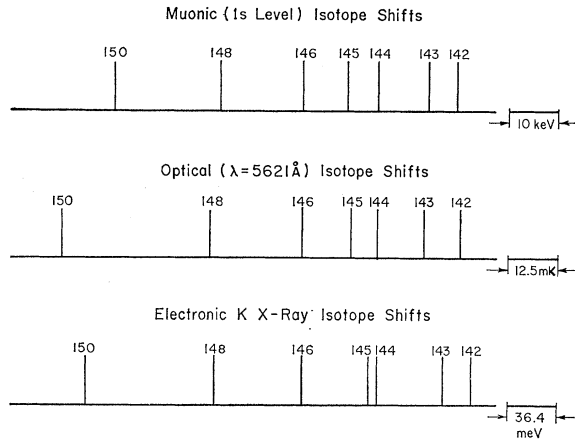


FIG. 9. Relative muonic (1s level), optical and electronic x-ray isotope shifts in Nd. The scale is shown at right. The optical data, from Ref. 39, are not corrected for specific-mass effects. The electronic x-ray data are from Ref. 40.

is more complicated than that of the neighboring even isotopes because of the presence of static quadrupole hyperfine effects. The ground state of ^{143}Nd has spin $\frac{7}{2}$ and a nuclear quadrupole moment of -0.48 b. The interaction of the muon with the nuclear quadrupole moment causes the $2p_{3/2}$ muon level to split into four components (the $2p_{1/2}$ level is not affected). Below the experimental spectrum of ^{143}Nd in Fig. 8 we have shown schematically the positions and relative strengths of these four components, as well as two other components due to isotopic impurities (see Table III). The calculated line width is in agreement with the observed value. The spectrum of ^{150}Nd is also more complicated, but in this case by dynamic quadrupole hyperfine effects (Fig. 8). Below the ^{150}Nd spectrum in this figure we have drawn schematically the principal components in the hyperfine structure, calculated in the manner discussed in the preceding paper. Note that this effect is absent from the ^{148}Nd spectrum. The anomalously large ^{148}Nd – ^{150}Nd isotope shift is clearly evident in this figure.

We have listed in Table VI the isotope shifts of the $K\alpha_1$, $K\alpha_2$, $L\alpha_1$, and $L\alpha_2$ lines of the even Nd isotopes. The effect of the dynamic $E2$ interaction is reflected in the values of the L isotope shifts, especially the very large 148–150 values. In Table VII, we list the 1s level shifts determined as described in Sec. IV; the estimated nuclear-polarization corrections, the calculated standard shifts $(\delta E)_{\text{std}}$, and the ratios of $(\delta E)_{\text{field}}/(\delta E)_{\text{std}}$. No nuclear-polarization corrections have been estimated for the odd isotopes.

In Fig. 9, we have plotted schematically the relative positions of the 1s level in the Nd isotopes. For comparison, the isotope shifts of the optical line $\lambda=5621$ Å as measured by Hansen *et al.*³⁹ are also shown in the same figure. The anomalous behavior of

the isotope shifts in Nd are strikingly apparent in all three measurements by different techniques. We will postpone a quantitative comparison of these results until the specific-mass effect has been discussed.

The $2p_{3/2}$ and $2p_{1/2}$ muon wave functions are slightly different inside the nucleus. The effect of this should appear as a small variation of the fine structure of the K and L lines, of the order of a small fraction of a keV between adjacent pairs of isotopes. To observe this variation, the dynamic $E2$ effect, which perturbs the $2p$ levels by different amounts, must be taken into account. The shifts of the $2p$ levels by this effect are listed in Table I. The measured and corrected fine-structure splittings of the K and L lines in the even Nd isotopes are presented in Table II, and plotted as a function of A in Fig. 10. In this figure, the circles are measured values, the crosses are corrected values, and the dotted line represents the values calculated for a Fermi distribution with $c \sim A^{1/3}$ and skin thickness t constant for all isotopes. The agreement between the corrected values and the values calculated under the assumption of constant t is very satisfactory.

We have measured the energy of the K and L lines for each Nd isotope with precision and accuracy adequate for the determination of two parameters of the nuclear charge distribution. We have therefore analyzed these results in terms of the parameters c and t of the Fermi distribution and the parameters α , t , and β [β fixed to values derived from $B(E2)$ mea-

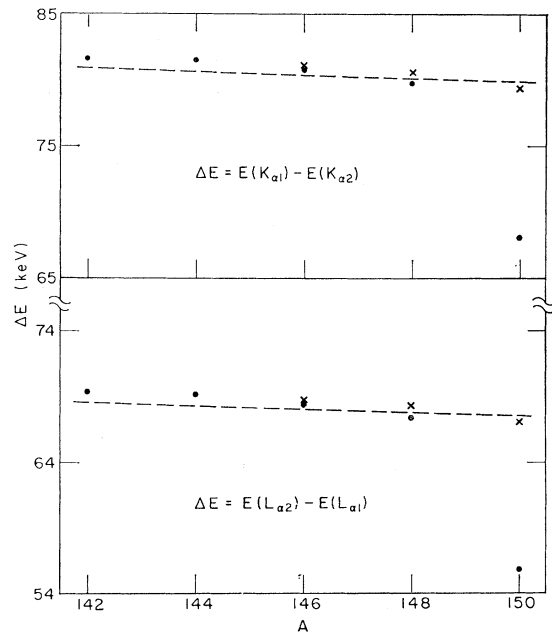


FIG. 10. Fine-structure splitting of the muonic K and L x rays of Nd versus mass number A . The circles are measured values; the crosses are values corrected for dynamic $E2$ effects. The dashed line represents the values calculated for a Fermi distribution with $c \sim A^{1/3}$ but t constant for all isotopes. Note that the fine-structure splitting is expected to decrease with A .

³⁹ J. E. Hansen, A. Steudel, and H. Walther, *Z. Physik* **203**, 296 (1967).

surements] of a deformed Fermi distribution [see Eqs. (5) and (6)]. The values obtained for these parameters are listed in Table X and plotted versus A in Fig. 11 for the spherical and in Fig. 12 for the deformed distributions. It is of great interest to note that even for these isotopes in the transition region, where the shape of nuclei changes from spherical to spheroidal, the skin thickness t does not vary a great deal. As a matter of fact, our results indicate that within the experimental uncertainties ($\pm 3-4\%$), we can consider the skin thickness as constant for the even Nd isotopes. For the deformed model, the skin thickness is generally smaller by a few percent than the corresponding values for the spherical model, as would be expected.

To extract the specific-mass effect in optical isotope shifts, we have plotted the relative isotope shifts of the $1s$ levels from our muonic measurements versus several optical isotope shifts^{39,41} as shown in Fig. 13. All four points which represent the isotope shifts between two adjacent ($e-e$) Nd isotopes (142-144, 144-146, 146-148, 148-150) lie on straight lines for each optical transition considered. From the intercept of the linear plot on the vertical axis, we can directly read the values of the specific-mass shifts. These mass effects together with the corrected optical shifts are summarized in Table XIII. It can be seen that the specific-mass shift varies over a wide range, as it depends on the particular electron transition involved.

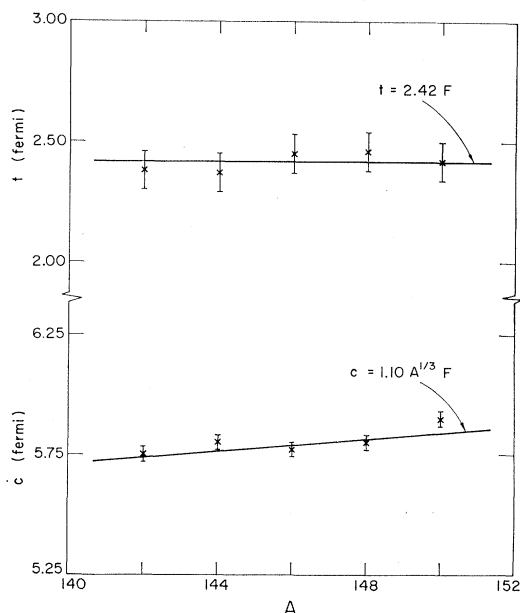


FIG. 11. Values of the parameters c and t of the Fermi distribution [Eq. (5)] plotted against mass number for the Nd isotopes. Note that the t values are constant within the error.

⁴⁰ S. Gerstenkorn and J. Helbert, *Compt. Rend.* **266**, 546 (1968).

⁴¹ S. K. Bhattacharjee, F. Boehm, and P. Lee, *Phys. Rev. Letters* **20**, 1295 (1968).

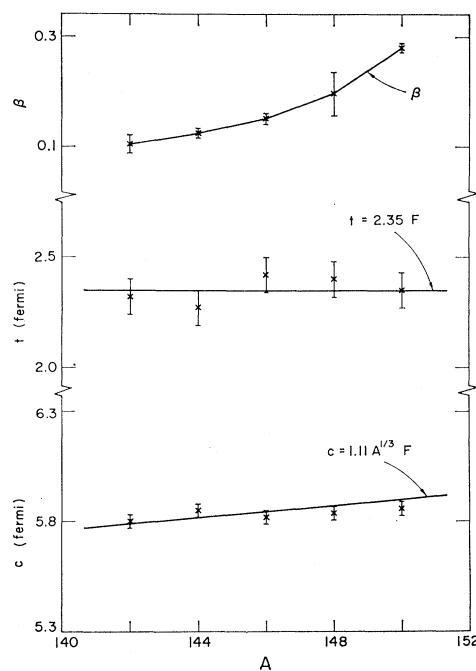


FIG. 12. Values of the parameters c , t , and β of the deformed Fermi distribution [Eq. (6)] plotted against mass number for the Nd isotopes. The values of β are from Refs. 16 and 17.

It is of interest that some recent preliminary results of a theoretical evaluation of the specific-mass shift in transitions of this type in Nd indicate a value of ~ 18 mK for the 5675 \AA line.⁴²

It is most important to compare the three totally different techniques of measuring the isotope shifts and to see whether the relative shifts and the ratios of $(\delta E)_{\text{field}}/(\delta E)_{\text{std}}$ thus obtained are in agreement. Table XIV shows such a comparison for Nd isotopes. The muonic results are from this work. The optical results for the 5675 \AA line are taken from Gerstenkorn *et al.*⁴⁰ The specific-mass correction from this work as listed in Table XIII have been applied to the observed optical shifts to yield the field effect. The values for the electronic x-ray shifts are from Bhattacharjee *et al.*⁴¹ Another electronic x-ray measurement of Nd isotopes by Sumbaev *et al.*⁴³ gives approximately the same values as those quoted. It can be seen that the over-all agreement is excellent. This indicates that the general assumptions used in extracting the specific-mass effect by muonic results are not unreasonable.

G. The Odd-Even Staggering

One of the most interesting features of the optical isotope shifts is the fact that lines of an odd-mass isotope are generally found to lie closer to the cor-

⁴² J. Bauche, *Compt. Rend.* **263**, 685 (1966).

⁴³ O. I. Sumbaev, E. V. Petrovich, V. S. Sykov, A. S. Ryl'nikov, and A. I. Grushko, *Yadern Fiz.* **5**, 544 (1967) [English transl.: *Soviet J. Nucl. Phys.* **5**, 387 (1967)].

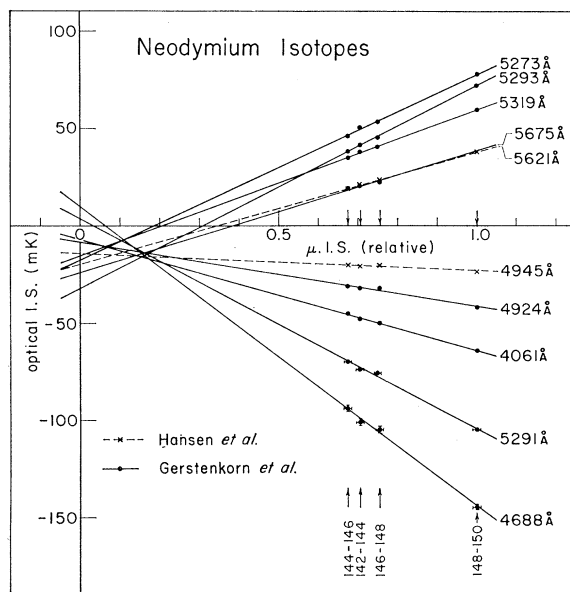


FIG. 13. Plot of optical isotope shifts versus relative muonic isotope shifts for the Nd isotopes. The optical data are from Refs. 39 and 40.

responding lines of its lighter even-mass neighbor than to those of its heavier one (odd-even staggering).

The first attempt to interpret the observed staggering effect was made by Wilets, Hill, and Ford⁴⁴ in 1953. They suggested that the effect was due to changes in the nuclear deformation, and argued that, on the basis of a simple deformed-shell model, the odd-mass isotopes were expected to be less deformed than the neighboring even-mass isotopes. However, neither experimental evidence nor more detailed calculations have shown that the nuclear deformations of odd-mass deformed nuclei are systematically less than those of even ones. Furthermore, most instances of pronounced staggering have been observed in or near spherical nuclei, rather than in deformed nuclei. In a recent theoretical paper,⁴⁵ Sorensen has shown that, on the basis of the pairing-plus-quadrupole model, near spherical odd-mass nuclei are expected to have smaller mean-square deformations than adjacent even-even isotopes by an amount sufficient to explain the observed staggering of the isotope shifts. Sorensen estimates that for a nucleus of mass ~ 150 , below the deformed region, this deformation effect would reduce the expected isotope shift by about 20% of the calculated standard isotope shift; that is, $\lambda_N \sim 0.8$ for the Nd isotopes.

In this work we have determined the odd-even staggering in the muonic isotope shifts in Cr, Mo, Sn, and Nd. The values of λ_N are listed in Table VIII, along with corresponding optical and electronic x-ray results. We note that the muonic values all cluster

⁴⁴ L. Wilets, D. L. Hill, and K. W. Ford, Phys. Rev. **91**, 1488 (1953).

⁴⁵ R. A. Sorensen, Phys. Letters **21**, 333 (1966).

around 0.7, except for the ⁹⁷Mo value. Moreover, the agreement between the results of the various techniques is reasonable, except for the unusually small electronic x-ray result in ¹⁴⁶Nd. The optical results in Mo and Nd have been calculated including the specific-mass corrections determined above, but the Sn results have been obtained using the specific-mass shift equal to 3.13 ± 0.25 mK which was determined from the comparison with electronic x-ray results.³² It is apparent, from the results quoted in Table XII, that without specific-mass corrections the optical values of λ_N for ⁹⁷Mo would be negative.

It should be pointed out that the muonic values of λ_N have been calculated without nuclear-polarization corrections, which could conceivably be quite different for odd and even nuclei when the structure of these nuclei is also quite different and could account for some of the differences.

VI. CONCLUSION

In this investigation we have studied many aspects of muonic isotope shifts in a wide range of nuclei. These include the shell-closure effects at neutron number equal to 28, the odd-even staggerings, and the field effects. From these systematic studies, together with their comparisons to optical and electronic x-ray isotope shifts, one gains insights on the fine variations of the charge distributions between isotopes. It has been emphasized in the literature that one of the main applications of muonic isotope shifts is to normalize the optical-isotope-shift results. However, this application was often questioned because the muonic shifts are model-dependent, while optical shifts are not. How these differences would limit the applicability of normalization or comparison of muonic shifts to optical shifts was extensively examined in this paper. Particularly, the factors which could affect the validity of the extraction of the specific-mass effects were studied and their orders of magnitude estimated. In the case of Nd, where accurate measurements of *K* and *L* x rays of five isotopes were made, the skin thickness was found to be constant within the experimental uncertainties. Furthermore the plots of optical shifts versus muonic shifts in Mo or Nd were found to be linear within the experimental uncertainties. Unfortunately, this is not the case for Sn. Notwithstanding, the comparison of the muonic measurements with several theoretical predictions shows a rather similar behavior of the shifts; the optical shift between ¹²²Sn-¹²⁴Sn as measured by Stacey seems to be at variance with both theory and muonic results. It is highly desirable to have both the optical isotope shifts of Sn further investigated and to have a series of measurements of isotope shifts between adjacent even-even Sn isotopes carried out by the electronic x-ray method. Should the future result of the electronic x-ray shift between ¹²²Sn-¹²⁴Sn confirm the behavior observed in the optical shift (that it is only

about half as large as the shift between ^{120}Sn - ^{122}Sn) it would certainly stimulate lively interest and discussion in its theoretical interpretation.

In general, the results of the three techniques of isotope shifts (i.e., muonic, optical, and electronic) are in fair agreement. However, when the conditions are favorable, the muonic x-ray method has the advantage that it yields, besides the changes of the rms radius, detailed information on the changes of more than one parameter of the nuclear charge distribution.

ACKNOWLEDGMENTS

The authors wish to express their profound appreciation to Dr. G. L. Rogosa of the U. S. Atomic

Energy Commission for his continued interest and efforts, and to Dr. K. Runge for his invaluable help in the early stages of the experiment. We particularly wish to take this opportunity to thank Dr. M. Y. Chen and Dr. L. Wilets for many enlightening discussions, and also to acknowledge our indebtedness to D. N. Stacey, J. E. Hansen, A. Steudel, H. Walther, and R. A. Sorensen for communicating their results to us prior to publication. We are indebted to William Hunt and the cyclotron crew for their efforts in operating the accelerator, and to A. M. Rushton for his help in running the experiment. We also wish to thank J. Ostrowsky and K. Ng for their assistance in the preparation of the targets.

Neutron-Proton Coincidence Measurement from the Neutron-Induced Breakup of the Deuteron

V. VALKOVIĆ, M. FURIĆ, D. MILJANIĆ, AND P. TOMAŠ

Institute "Ruder Bošković," Zagreb, Yugoslavia

(Received 12 November 1969)

A method for measuring neutron-charged-particle coincidences from the 14.4-MeV neutron-induced reaction has been developed. The $n+d \rightarrow p+n+n$ reaction has been studied by the coincidence detection of the outgoing proton and neutron. The cross section has been measured as a function of five independent kinematic variables. A contribution of neutron-proton quasifree scattering has been observed. The cross section for $\Theta_n = \Theta_p = 30^\circ$ is found to be $\sigma = 37.5 \pm 5.8$ mb/sr². This result is in fair agreement with the data for proton-proton quasifree scattering from the $p+d \rightarrow p+p+n$ reaction. The possibility of obtaining a proper a_{nn} value is discussed.

I. INTRODUCTION

NUCLEAR reactions with three particles in the final state have been studied with increasing interest in recent years. Special attention has been paid to reactions with three nucleons in the final state: (1) $n+d \rightarrow p+n+n$ and (2) $p+d \rightarrow p+p+n$. Since free neutron targets are not yet available, reaction (1) is the simplest one, giving hope to obtain information on the neutron-neutron force.

In spite of considerable experimental difficulties involved in the investigation of neutron-induced reactions, reaction (1) has been studied by many groups.¹⁻⁶ However, only the one-particle energy spectra and angular distributions have been measured. The peaks in the energy spectra have been interpreted as a consequence of the neutron-neutron and the neutron-proton final-state interaction. In order to extract the neutron-

neutron scattering length, the measured single counter energy spectra have been analyzed using the Watson-type⁷ theories, impulse approximation,⁸ Amado approach,⁹ and the graph-summation method.¹⁰

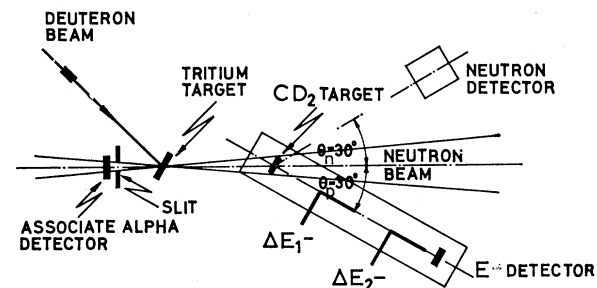


FIG. 1. Positions of the proton detector (counter telescope) and the neutron detector with respect to the neutron beam. The neutron beam was defined by a slit in front of the associated α -particle detector.

¹ K. Ilakovac, L. G. Kuo, M. Petravić, I. Šlaus, and P. Tomaš, Phys. Rev. Letters **6**, 356 (1961).

² M. Cerineo, K. Ilakovac, I. Šlaus, P. Tomaš, and V. Valković, Phys. Rev. **133**, B948 (1964).

³ E. Bar-Avraham, R. Fox, J. Portath, G. Adam, and G. Frieder, Nucl. Phys. **B1**, 49 (1967).

⁴ A. Bond, Nucl. Phys. **A120**, 183 (1968).

⁵ S. Shirato and N. Koori, Nucl. Phys. **A120**, 387 (1968).

⁶ H. Grössler and R. Honecker, Nucl. Phys. **A136**, 446 (1968), and references therein.

⁷ K. M. Watson, Phys. Rev. **88**, 1163 (1952).

⁸ G. F. Chew, Phys. Rev. **80**, 196 (1950); G. F. Chew and F. E. Low, *ibid.* **113**, 1640 (1959).

⁹ R. Amado, Phys. Rev. **132**, 485 (1963); R. Aaron, R. Amado, and Y. Yam, *ibid.* **140**, B1291 (1965); R. Aaron and R. Amado, *ibid.* **150**, 857 (1966).

¹⁰ V. V. Komarov and A. M. Popova, Nucl. Phys. **54**, 278 (1964).